Bioorganic Chemistry 82 (2019) 86–99

Contents lists available at ScienceDirect

Bioorganic Chemistry

journal homepage: www.elsevier.com/locate/bioorg

Design, synthesis, modeling studies and biological evaluation of thiazolidine derivatives containing pyrazole core as potential anti-diabetic PPAR-γ agonists and anti-inflammatory COX-2 selective inhibitors

Khaled R.A. Abdellatif[a,b,*], Wael A.A. Fadaly[a], Gehan M. Kamel[c], Yaseen A.M.M. Elshaier[d], Mohammed A. El-Magd[e]

[a] Pharmaceutical Organic Chemistry Department, Faculty of Pharmacy, Beni-Suef University, Beni-Suef, Egypt
[b] Pharmaceutical Sciences Department, Ibn Sina National College for Medical Studies, Jeddah 21418, Saudi Arabia
[c] Pharmacology Department, Faculty of Veterinary, Cairo University, Cairo, Egypt
[d] Pharmaceutical Organic Chemistry Department, Faculty of Pharmacy, Al-Azhar University, Assuit 71524, Egypt
[e] Anatomy Department, Faculty of Veterinary Medicine, Kafrelshiekh University, Kafrelshiekh, 33516, Egypt

ARTICLE INFO

Keywords:
Thiazolidine
Pyrazole
Cyclooxygenase-2 inhibitors
Anti-inflammatory
Anti-diabetic
PPARγ

ABSTRACT

Nowadays, diabetes and its associated inflammatory complications are important public health problems worldwide. Market limitations of drugs with dual actions as anti-inflammatory (AI) and anti-diabetic have been led to a temptation for focusing on the discovery and development of new compounds with potential AI and anti-diabetic activities. Herein, we synthesized two new series containing pyrazole ring with vicinal diaryl rings as selective COX-2 moiety and thiazolidindione (series **12a-f**) or thiazolidinone (series **13a-f**) as anti-diabetic moiety and the two moieties were linked together with methylene or methylenehydrazone functionality. The two series were evaluated for their COX inhibition, AI activity and ulcerogenic liability and for the anti-diabetic activity; **12a-f** and **13a-f** were assessed *in vitro* against α-glucosidase, β- glucosidase, *in vivo* hypoglycemic activity (one day and 15 days studies) in addition to PPARγ activation study. Four compounds (**12c**, **12f**, **13b** and **13f**) had higher COX-2 S.I. (8.69–9.26) than the COX-2 selective drug celecoxib (COX-2 S.I. = 8.60) and showed the highest AI activities and the lowest ulcerogenicity than other derivatives. Also, two thiazolidindione derivatives **12e** and **12f** and two thiazolidinone derivatives **13b** and **13c** showed higher inhibitory activities against *α*- and *β*-glucosidase (% inhibitory activity = 62.15, 55.30, 65.37, 59.08 for α-glucosidase and 57.42, 60.07, 58.19, 66.90 for β-glucosidase respectively) than reference compounds (acarbose with % inhibitory activity = 49.50 for α-glucosidase and D-saccharic acid 1,4-lactone monohydrate with % inhibitory activity = 53.42 for β-glucosidase) and also showed good PPAR-γ activation and good hypoglycemic effect in comparison to pioglitazone and rosiglitazone. Moreover, Shape comparison and docking studies were carried out to understand their interaction and similarity with standard drugs.

1. Introduction

Diabetes is the most serious life style disorder metabolic disease that attacks the world at an alarming wide spread rate. It is categorized as Type-I and Type-II which occurred due to insulin resistance in body tissues and its occurrence is aided by several factors such as obesity, stress, diet and lack of physical activity [1].

Thiazolidin-4-one ring system [2,3] and thiazolidindione s (TZDs, glitazones) have been widely used for management of Type-II diabetes mellitus [4]. TZDs, agonists of the peroxisome proliferator activated receptor-γ (PPAR-γ), [5–8] are kind of anti-hyperglycemic agents that reduce insulin resistance and improve insulin action thereby keeping normoglycemia and potentially preserving β-cell function [9–14]. Recently, TZDs are considered also to have a role in the treatment of some inflammatory diseases [15]. There is an increasing evidence that inflammation is responsible for the pathogenesis of diabetes and associated complications [16,17]. Therefore, drugs with anti-inflammatory properties such as TZDs can possibly decrease the risk of developing diabetes and diabetes-induced inflamed problems. Pioglitazone (**1**), rosiglitazone (**2**) and troglitazone (**3**) (Fig. 1) are common clinical agents from TZDs act as anti-diabetic by enhancing insulin sensitivity in liver, muscles and fat tissues and by counteracting insulin resistance [18–21].

* Corresponding author at: Pharmaceutical Organic Chemistry Department, Faculty of Pharmacy, Beni-Suef University, Beni-Suef, Egypt.
E-mail address: khaled.ahmed@pharm.bsu.edu.eg (K.R.A. Abdellatif).

https://doi.org/10.1016/j.bioorg.2018.09.034
Received 9 August 2018; Received in revised form 22 September 2018; Accepted 24 September 2018
Available online 25 September 2018
0045-2068/

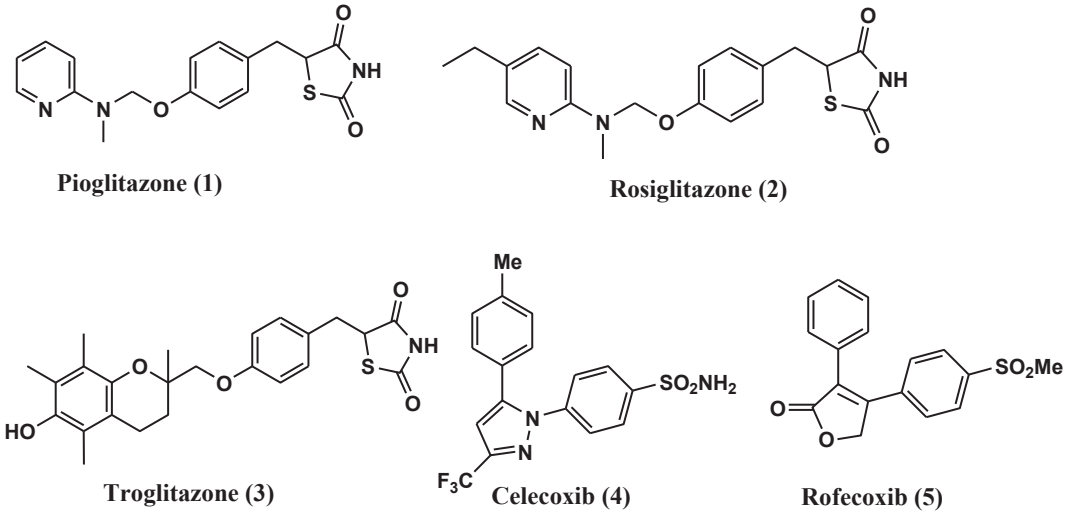

Fig. 1. Chemical structures of thiazolidindione anti-diabetic pioglitazone (**1**), rosiglitazone (**2**) and troglitazone (**3**) and the selective cyclooxygenase-2 inhibitors celecoxib (**4**) and rofecoxib (**5**).

PPAR-γ is a member of nuclear receptors super family that regulate the expression of gene included in lipid and glucose metabolism [22–24]. PAR-γ is involved in the regulation of immune and anti-inflammatory response through modulation of macrophage activation and repression of pro-inflammatory genes, such as iNOS and cyclooxygenase (COX) resulting in inhibition of expression of cytokines and nuclear factor kappa-B (NFkB) pathway that have been found to play a critical role in the development of micro-vascular diabetic complications, including nephropathy, the main cause of diabetes-induced renal failure [25–28].

On the other hand, non-steroidal anti-inflammatory drugs (NSAIDs) are among the most widely used therapeutics through their anti-inflammatory, antipyretic and analgesic activities [29]. Selective inhibition of the inducible cyclooxygenase-2 (COX-2) isozyme in the periphery provided a useful drug design concept that resulted in the development of effective anti-inflammatory (AI) drugs that were devoid of adverse gastrointestinal ulcerogenicity commonly accompanied the use of NSAIDs [30]. Coxibs, one of the most common selective COX-2 inhibitors, are diarylheterocycles in which two vicinal aryl moieties are attached to a central five-membered ring as pyrazole in celecoxib (**4**) [31] and furanone in rofecoxib (**5**) [32]. Also, one of the two aryl rings is substituted at para position with one COX-2 pharmacophoric moiety either aminosulfonyl (SO_2NH_2) or methanesulfonyl (SO_2CH_3) moiety (Fig. 1).

Molecular hybridization, one of the most efficient strategies in the drug design medicinal chemistry, is based on the combination of pharmacophoric moieties of different bioactive substances to produce a new hybrid compound with improved affinity and efficacy when compared to the parent drugs. Furthermore, this pharmacophoric hybridization method is used for the synthesis of novel bioactive hybrid drug with dual biological activities [33]. Also, hybridization of two bioactive compounds with complementary pharmacophoric purposes or with different mechanisms of action frequently gives synergistic effects [34]. Guided by the above mentioned information, our group was encouraged to design rosiglitazone / celecoxib hybrid anti-diabetic/ anti-inflammatory analogues **12a-f** and **13a-f** through synthesis of heterocycles containing vicinal diaryl pyrazole core as central ring (COX-2 scaffold) bearing thiazolidindione or thiazolidinone moiety (PPAR-γ pharmacophoric agonist) to discover new candidates that may be of importance in designing new compounds that possess both anti-diabetic and anti-inflammatory activities. The structure of the new derivatives **12a-f** and **13a-f** maintains the Y shape of coxibs with pyrazole core like celecoxib (**4**) and the acidic head thiazolidindione pharmacophore of rosiglitazone (**2**) or its bioisostere thiazolidinone moiety was incorporated in pyrazole C4 with different linkers. Also, a COX-2 pharmacophore (SO_2Me) was *para*-substituted to phenyl ring attached to pyrazole C1 to maintain COX-2 selectivity (Fig. 2).

Based on the aforementioned information, and in continuation of our previous work [35–38], we now describe the synthesis, *in vitro* evaluation as COX-1/COX-2 inhibitors, *in vivo* AI activity and ulcerogenic liability of thiazolidine derivatives containing pyrazole core **12a-f**, and **13a-f**. Also, the *α*- and *β*- *in vitro* glucosidase inhibition activity, *in vitro* PPAR-γ assay and the *in vivo* anti-diabetic evaluation will be described. Additionally, the 3D shape similarity and docking studies will be illustrated to understand correctly about structure activity relationship and ligand receptor interactions.

2. Results and discussion

2.1. Chemistry

The hydrazones **8a-f** were synthesized *via* condensation of the acetophenone derivatives **6a-f** with the 4-methanesulfonylphenyl hydrazine hydrochloride **7** under reflux conditions according to a reported procedure [39]. Applying Vilsmeier-Haack reaction (dimethylformamide and phosphorus oxychloride) to hydrazones **8a-f** afforded the respective pyrazole aldehydes **9a-f**. Condensation of the key aldehydes **9a-f** with 2,4-thiazolidindione **11** in absolute ethanol and few drops of pipridine afforded the target thiazolidindione -pyrazole derivatives **12a-f**. The structure of **12a-f** was confirmed by appearance of a singlet for CH═C− proton at 7.38–7.56 ppm and a broad singlet for NH-TZD proton at 12.29–12.39 ppm in ^{1}H NMR spectra followed by the presence of peaks at 3244–3117 cm^{-1} (NH), 1755–1744 (C═O) and 1617–1613 (−CH═C) in the IR spectrum. The other series of the target compounds **13a-f** was obtained via condensation of the pyrazole aldehydes **9a-f** with thiosemicarbazide in ethanol to give the pyrazolyl thiosemicarbazone intermediates **10a-f** which upon reaction with chloroacetic acid in glacial acetic acid and sodium acetate undergo cyclization into the final target thiazolidin-4-one derivatives **13a-f**. The structure of **13a-f** was confirmed by appearance of a singlet for (CH═C−) proton at 8.28–8.49 ppm and a singlet for thiazolidine-4-one (−CH_2−) protons at 3.62–3.94 ppm in ^{1}H NMR spectra followed by the presence of peaks at 3203–3431 cm^{-1} (NH), 1711–1731 (C═O) and 1596–1644 (−CH═C) in the IR spectrum (Scheme 1).

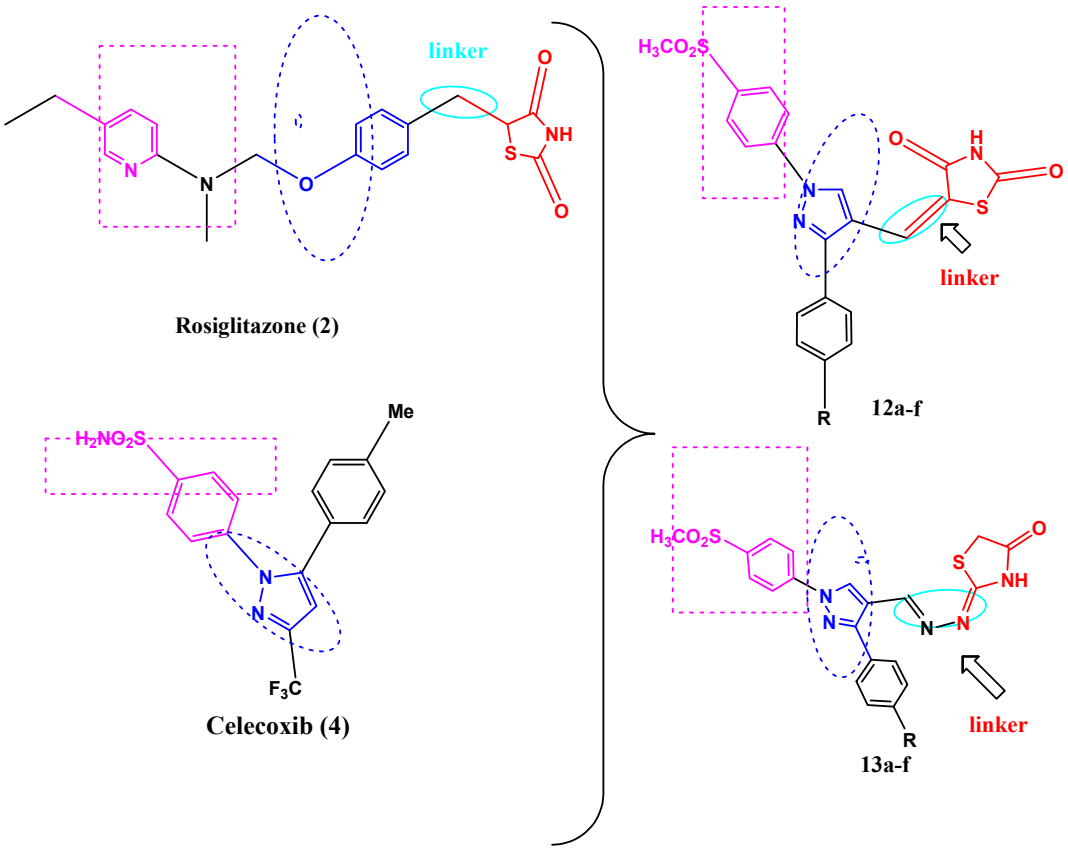

Fig. 2. Chemical structures of rosiglitazone (**2**), celecoxib (**4**), the target thiazolidindione s (**12a-f**) and the target thiazolidinones (**13a-f**).

2.2. Biological evaluation

2.2.1. Ant-inflammatory

2.2.1.1. In vitro cyclooxygenase inhibition assay. The *in vitro* COX-1/COX-2 isozyme inhibition studies evaluated the ability of the target thiazolidine-pyrazole derivatives **12a-f** and **13a-f** to inhibit ovine COX-1 and human recombinant COX-2 using an enzyme immunoassay (EIA) [40]. The data (Table 1) showed that the target compounds possessed week inhibitory activities against COX-1 isozyme (IC_{50} = 3.55–10.87 μM range) but showed high COX-2 isozyme inhibitory activities (IC_{50} = 0.48–1.92 μM range) with COX-2 selectivity indexes in the range of 5.66 to 9.26 in comparison to the COX-2 selective reference drug celecoxib (COX-1 IC_{50} = 7.23 μM, COX-2 IC_{50} = 0.84 μM and S.I. = 8.60). Among all derivatives **12a-f** and **13a-f**, the methoxy derivative **12f** was highly potent against COX-2 (IC_{50} = 0.88 μM) and had the highest COX-2 selectivity index (S.I. = 9.26) while the chloro derivative **12b** had the lowest COX-2 selectivity index (S.I. = 5.66). Similarly, within the thiazolidinone derivatives **13a-f**, the methoxy derivative **13f** was highly potent against COX-2 (IC_{50} = 0.62 μM) and had the highest COX-2 selectivity index (S.I. = 8.85).

2.2.1.2. In vivo anti-inflammatory activity. The *in vivo* anti-inflammatory activity of the target compounds **12a-f** and **13a-f** and celecoxib as a reference drug was determined using carrageenan-induced rat paw edema assay according to the reported procedure [41] using a dose of 50 mg/kg body weight. The anti-inflammatory activity was then calculated based on paw-volume changes at 1, 3 and 5 h after carrageenan injection as presented in Table 2. It was noted that all compounds significantly decreased inflammation as compared with carrageenan at all-time intervals. A comparable study of the anti-inflammatory activity of the test compounds relative to celecoxib as a reference drug at the different time intervals showed that; after 1 h, they showed moderate to good anti-inflammatory activity (AI = 55.34–82.51%) in comparison to celecoxib (AI = 41.73%). After 3 h, the anti-inflammatory activity was decreased (AI = 39.88–76.49%) except for two derivatives **13e** and **13f**, the anti-inflammatory activity was increased (AI = 70.71 and 97.68% respectively and AI for celecoxib = 80.38%). while after 5 h, the anti-inflammatory activity was maintained without considerable change (AI = 39.88–80.15%) and (AI = 68.78, 97.68% for **13e**, **13f** respectively and AI for celecoxib = 89.00%). The methoxy derivatives (**12f** and **13f**), the most COX-2 selective derivatives (S.I. = 9.26 and 8.85 respectively), showed the highest AI activities (after 1 h, AI = 82.34 and 81.15%, after 3 h, AI = 79.00 and 97.68% and after 5 h, AI = 80.15 and 97.68% respectively).

Furthermore, the dose causing 50% edema inhibition (ED_{50}) was determined for the most potent AI derivatives **12b**, **12bc**, **12f**, **13b**, **13c**, **13e** and **13f** in comparison to celecoxib. They revealed good anti-inflammatory activities (ED_{50} = 5.63–79.12 μmol/kg), while **12f** was slightly more potent (ED_{50} = 79.12 μmol/kg) than celecoxib (ED_{50} = 82.2 μmol/kg), **13e** showed the best ED_{50} (5.63) with more than 14 folds potency of celecoxib (Table 3).

2.2.1.3. Ulcerogenic liability. Also, the ulcerogenic effect (ulcer index) for the most potent derivatives **12b**, **12bc**, **12f**, **13b**, **13c**, **13e** and **13f** was determined using 50 mg/kg dose in comparison to celecoxib (50 mg/kg dose) and small dose of ibuprofen (120 μmol/kg) [42]. The results revealed that all tested compounds were significantly less ulcerogenic (ulcer indexes = 2.62–5.11) than ibuprofen (ulcer index = 20.25) and were of comparable ulcerogenicity to the non-ulcerogenic reference drug celecoxib (ulcer index = 2.93). Compound **13e** with the best ED_{50} (5.63) was the least ulcerogenic derivative (ulcer index = 2.62) even less ulcerogenic than the non-ulcerogenic reference drug celecoxib. Also, the most COX-2 selective derivatives **12f** and **13f** showed low ulcerogenic effects (ulcer index = 3.97 and 3.12 respectively) (Table 4).

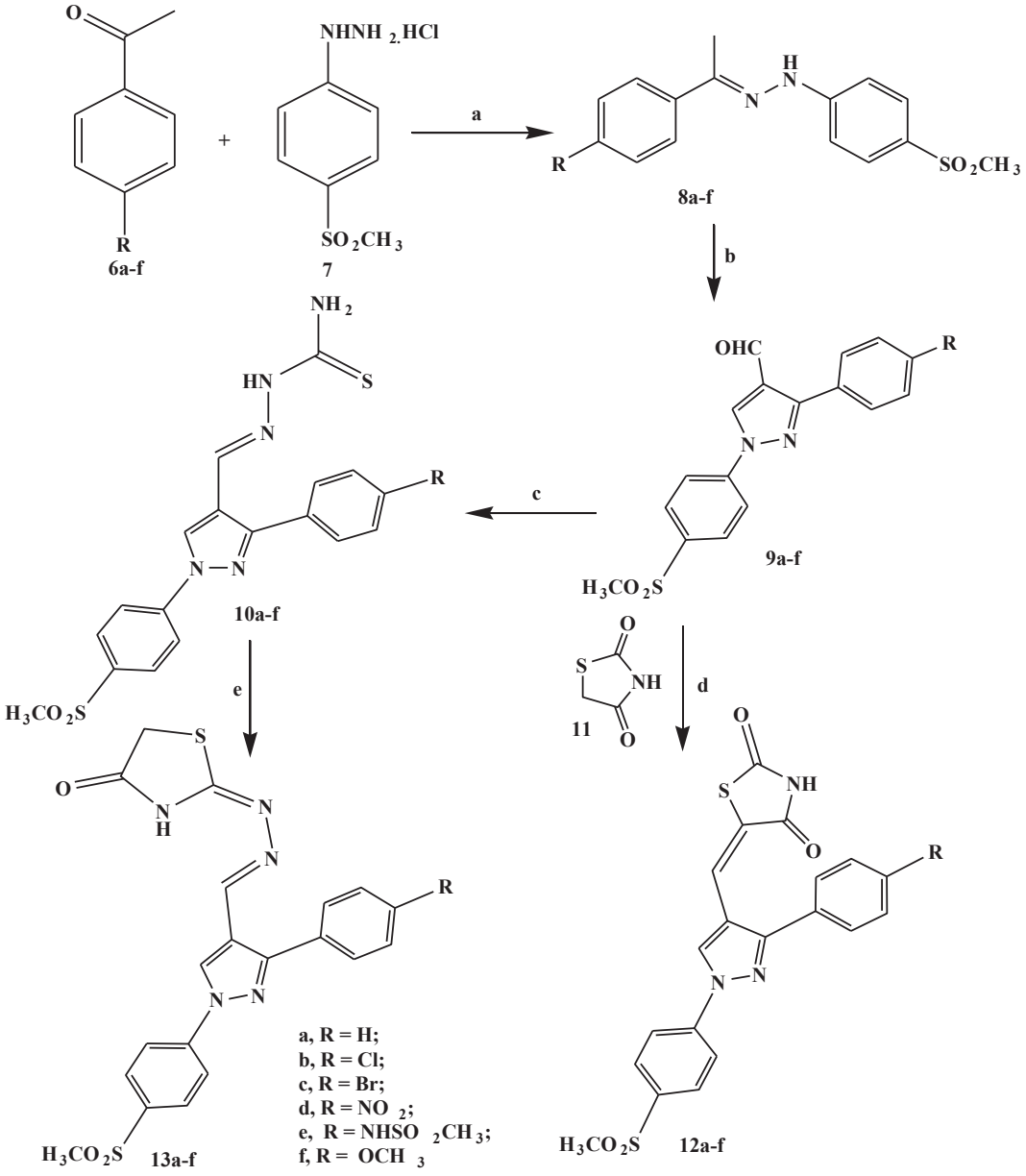

Scheme 1. Synthesis of the target compounds **12a-f** and **13a-f**.

Table 1
In vitro COX-1 and COX-2 inhibitory activity of the target derivatives **12a-f**, **13a-f** and reference drug celecoxib.

Compound	COX-1 IC_{50} (μM)[a]	COX-2 IC_{50} (μM)[a]	COX-2 S.I.[b]
12a	3.55	0.48	7.39
12b	10.87	1.92	5.66
12c	5.77	0.63	9.15
12d	6.32	0.84	7.52
12e	4.22	0.66	6.39
12f	8.15	0.88	9.26
13a	3.81	0.61	6.24
13b	8.52	0.98	8.69
13c	4.75	0.61	7.78
13d	5.17	0.82	6.30
13e	9.39	1.55	6.05
13f	5.49	0.62	8.85
Celecoxib	7.23	0.84	8.60

[a] The concentration of test compound produce 50% inhibition of COX-1, COX-2 enzyme, the result is the mean of two values.
[b] The *in vitro* COX-2 selectivity index (COX-1/COX-2).

2.2.2. Ant-diabetic activity

2.2.2.1. In vitro α-glucosidase/β-glucosidase inhibitory activity. The *in vitro* α-glucosidase/β-glucosidase inhibition studies evaluated the ability of the target compounds (thiazolidindione **s 12a-f** and thiazolidinone **13a-f**) to inhibit the effect of α-glucosidase [43] and β-glucosidase [44] as carbohydrate-digesting enzymes. The data listed in Table 5 revealed that the target compounds had wide range of inhibitory activities against both α-glucosidase and β-glucosidase (% inhibitory activity = 19.32–65.37 for α-glucosidase in comparison to acarbose which had 49.5% while % inhibitory activity = 20.79–66.90 for β-glucosidase in comparison to D-saccharic acid 1,4-lactone monohydrate which had 53.42%). Within the thiazolidindione series **12a-f**, two derivatives **12e** and **12f** showed higher inhibitory activities than reference compounds (% inhibitory activity = 62.15, 55.30 for α-glucosidase and 57.42, 60.07 for β-glucosidase respectively). Also, within the thiazolidinone series **13a-f**, two derivatives **13b** and **13c** showed higher inhibitory activities than reference compounds (% inhibitory activity = 65.37, 59.08 for α-glucosidase and 58.19, 66.90 for β-glucosidase respectively).

Table 2
In vivo anti-inflammatory activity of the target compounds **12a-f**, **13a-f** and reference drug celecoxib.

Compound No.	Mean value of paw edema thickness (cm) ± SEM (% of inhibition)		
	1 h	3 h	5 h
12a	2.61 ± 0.0057 (55.68%)	2.93 ± 0.1154 (43.54%)	2.95 ± 0.0057 (42.60%)
12b	1.43 ± 0.01 (75.72%)	1.83 ± 0.01 (64.74%)	1.83 ± 0.0057 (64.74%)
12c	1.05 ± 0.01 (82.17%)	1.38 ± 0.01 (73.41%)	1.44 ± 0.0057 (72.25%)
12d	2.53 ± 0.0054 (57.04%)	2.52 ± 0.0115 (51.44%)	2.55 ± 0.0152 (50.86%)
12e	2.42 ± 0.005** (58.91%)	2.63 ± 0.023** (49.32%)	2.66 ± 0.005** (48.74%)
12f	1.04 ± 0.01 (82.34%)	1.09 ± 0.01 (79%)	1.03 ± 0.0057 (80.15%)
13a	2.04 ± 0.0055 (65.36%)	2.14 ± 0.0051 (58.76%)	2.34 ± 0.0173 (54.91%)
13b	1.03 ± 0.01 (82.51%)	1.22 ± 0.01 (76.49%)	1.30 ± 0.0057 (74.95%)
13c	1.32 ± 0.01 (77.58%)	1.72 ± 0.01 (66.85%)	1.74 ± 0.0057 (66.47%)
13d	2.63 ± 0.01*** (55.34%)	3.12 ± 0.01*** (39.88%)	3.12 ± 0.01*** (39.88%)
13e	2.02 ± 0.01 (65.70%)	1.52 ± 0.011 (70.71%)	1.62 ± 0.011 (68.78%)
13f	1.11 ± 0.01 (81.15%)	0.12 ± 0.0057 (97.68%)	0.12 ± 0.0152 (97.68%)
Celecoxib	3.03 ± 0.0057 (41.73%)	1.02 ± 0.152 (80.38%)	0.11 ± 0.01 (89%)

Values represent means ± SEM of four animals for each group.
** Means significant difference with celecoxib at $p < 0.05$.
*** Means highly significant difference with celecoxib at $p < 0.005$.

Table 3
ED_{50} for the most active derivatives **12b**, **12c**, **12f**, **13b**, **13c**, **13e**, **13f** and reference drug celecoxib.

Compound	% of inhibition			ED_{50} (mg/kg)[a]	ED_{50} (μmol/kg)[a]
	10 mg/kg	25 mg/kg	50 mg/kg		
12b	43.22	58.36	77.54	18	39.21
12c	3.88	30.22	72.18	37	73.70
12f	2.46	29.92	69.19	36	79.12
13b	45.15	55.54	77.81	15	31.71
13c	18.31	34.69	71.03	33	63.95
13e	53.85	62.23	77.69	3	5.63
13f	39.46	58.92	91.00	18	38.37
Celecoxib	17.00	39.00	80.00	31.3	82.20

[a] Inhibitory activity in a carrageenan-induced rat paw edema assay. The results are expressed at 3 h after oral administration of the test compounds.

Table 4
Ulcerogenic liability for the most active derivatives **12b**, **12c**, **12f**, **13b**, **13c**, **13e**, **13f** and reference drugs celecoxib and ibuprofen.

Compound	Average severity	Average no of ulcer[a]	% incidence 10	Ulcer index
12b	0.66 ± 0.038	0.5 ± 0.018***	4	5.11
12c	0.74 ± 0.053	0.4 ± 0.022***	3	4.13
12f	0.54 ± 0.027	0.4 ± 0.02 ***	3	3.97
13b	0.50 ± 0.026***	0.4 ± 0.013***	4	4.83
13c	0.35 ± 0.018***	0.4 ± 0.016***	3	3.87
13e	0.46 ± 0.019***	0.3 ± 0.015***	2	2.62
13f	0.83 ± 0.042***	0.3 ± 0.016	2	3.12
Celecoxib	0.63 ± 0.037	0.3 ± 0.017	2	2.93
Ibuprofen	2.25 ± 0.13	8.0	10	20.25

[a] Values represent means ± SEM of ten animals for each group.
*** Means significant difference with celecoxib at $p < 0.001$.

2.2.2.2. In vitro PPAR-γ activation. The two thiazolidindione derivatives **12e** and **12f** and the two thiazolidinone derivatives **13b** and **13c** that showed higher inhibitory activities against α-glucosidase and β-glucosidase were subjected to further study [7] to detect their effect on PPAR-γ activation in comparison to the reference drugs pioglitazone (**1**) and rosiglitazone (**2**). The four compounds (**12e**, **12f**, **13b** and **13c**) induced PPAR-γ activation and showed 52.11%, 59.63%, 63.15%, and 55.24% PPAR-γ transactivation respectively as compared to pioglitazone (76.72%) and rosiglitazone (82.6%) (Fig. 3).

Table 5
In vitro α-glucosidase and β-glucosidase inhibitory activity of the target derivatives **12a-f**, **13a-f** and reference drugs acarbose and D-saccharic acid 1,4-lactone monohydrate.

Compound	% Inhibitory activity ± SEM	
	α-Glucosidase	β-Glucosidase
12a	31.45 ± 2.47	26.11 ± 1.90
12b	28.11 ± 2.52	31.05 ± 2.0
12c	47.24 ± 3.01	48.49 ± 2.85
12d	39.28 ± 2.74	44.15 ± 2.74
12e	62.15 ± 4.38	57.42 ± 4.04
12f	55.3 ± 4.02	60.07 ± 4.35
13a	19.32 ± 1.02	34.05 ± 2.11
13b	65.37 ± 5.4	58.19 ± 5.24
13c	59.08 ± 4.74	66.9 ± 6.01
13d	27.8 ± 2.24	20.79 ± 2.63
13e	40.5 ± 4.9	43.12 ± 4.17
13f	31.21 ± 3.77	27.38 ± 2.93
Acarbose	49.5 ± 1.73	–
D-Saccharic acid 1,4-lactone monohydrate	–	53.42 ± 2.16

– Inhibitory activity (%) = (1 − At/Ac) × 100, where, "At" is the absorbance in the presence of test substance and "Ac" is the absorbance of control.
– Data was obtained from three independent experiments and each experiment was performed in triplicates.

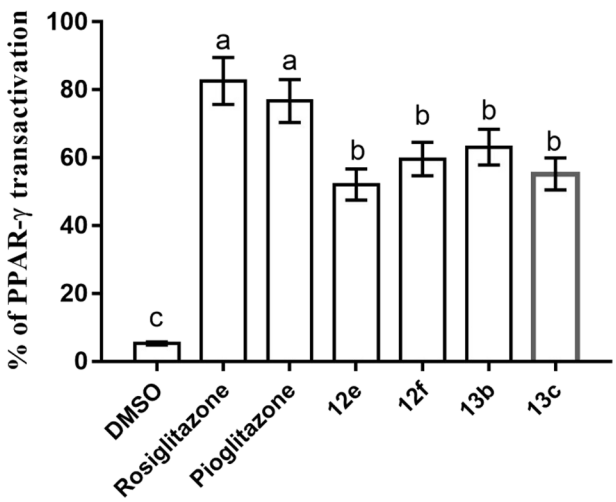

Fig. 3. *In vitro* PPAR-γ transactivation assay of **12e**, **12f**, **13b**, **13c** and reference drugs pioglitazone (1) and rosiglitazone (**2**).

Table 6
Hypoglycemic activity of the target compounds (**12a-f** and **13a-f**) and reference drug rosiglitazone (one day study).

Compd	Blood glucose level (mg/dl)				
	0 h	2 h	4 h	6 h	12 h
12a	307.29 ± 4.02	271.86 ± 1.39****	230.87 ± 0.226****	192.69 ± 0.935****	163.486 ± 3.478****
12b	276.52 ± 0.868	244.23 ± 0.32****	213.553 ± 1.439****	189.116 ± 1.505****	151.086 ± 0.600****
12c	280.42 ± 0.24	239.55 ± 1.00****	210.596 ± 0.070****	290.096 ± 0.172****	188.99 ± 1.650****
12d	270.59 ± 0.308	239.39 ± 0.91****	208.626 ± 1.247****	180.206 ± 0.325****	166.72 ± 0.1053****
12e	254.33 ± 1.275	231.35 ± 0.56****	202.89 ± 0.633****	179.276 ± 0.501****	144.16 ± 1.950****
12f	231.81 ± 0.622	210.48 ± 0.85****	196.89 ± 1.187****	175.483 ± 1.115****	167.823 ± 1.602****
13a	321.59 ± 0.895	309.58 ± 1.00	310.716 ± 0.160	300.156 ± 1.799	291.53 ± 0.893
13b	279.263 ± 1.51	243.55 ± 0.960****	231.26 ± 0.681****	201.386 ± 1.000****	187.496 ± 1.114****
13c	261.45 ± 1.005	231.47 ± 1.11****	214.486 ± 1.110****	190.783 ± 0.759****	175.746 ± 1.605****
13d	254.14 ± 1.276	228.46 ± 1.150****	204.723 ± 1.30****	175.786 ± 0.482****	162.98 ± 2.233****
13e	311.026 ± 0.45	219.84 ± 1.032****	220.076 ± 0.361****	202.306 ± 1.593****	175.786 ± 1.275****
13f	281.95 ± 1.172	231.88 ± 0.98****	232.62 ± 2.204****	206.163 ± 1.130****	180.566 ± 1.225****
Diabetic control	319.446 ± 0.19	318.63 ± 1.98****	314.253 ± 1.935****	315.39 ± 2.175****	321.136 ± 0.840****
Rosiglit-azone	308.956 ± 0.52	164.89 ± 0.60****	144.72 ± 0.998****	144.69 ± 0.951****	118.826 ± 1.379****

Values represent means ± SEM of four animals for each group.
**** Means significant difference with reference drug at $p < 0.0001$ versus 0 h.

2.2.2.3. In vivo hypoglycemic study. The *in vivo* blood glucose lowering effect of the target compounds **12a-f** and **13a-f** and rosiglitazone (**2**) as a reference drug was determined using alloxan induced diabetic rats according to the reported procedure [45] through one day and fifteen days studies.

2.2.2.3.1. One day study. Blood samples were taken from all animals at 0, 2, 4, 6 and 12 h. The data obtained (Table 6) indicated that all compounds **12a-f** and **13a-f** had significant hypoglycemic effect when compared to the reference drug rosiglitazone at all-time intervals. Also, it was clear that the hypoglycemic effect increased with time (12 > 6 > 4 > 2 h). Compounds showed higher inhibitory activities against α-glucosidase and β-glucosidase (thiazolidindione derivatives **12e** and **12f** and thiazolidinone derivatives **13b** and **13c**) showed good hypoglycemic effect (low blood glucose level) relative to rosiglitazone at the different time intervals; at 2 h, the blood glucose levels were 231.35, 210.48, 243.55 and 231.47 mg/dl respectively relative to rosiglitazone = 164.89. At 4 h, the blood glucose levels were 202.89, 196.89, 231.26 and 214.49 mg/dl respectively relative to rosiglitazone = 144.72. While at 6 h, the blood glucose levels were 179.28, 175.48, 201.39 and 190.78 mg/dl respectively relative to rosiglitazone = 144.69, the blood glucose levels at 12 h were the least (144.16, 167.82, 187.50 and 175.75 mg/dl respectively relative to rosiglitazone = 118.83).

2.2.2.3.2. Fifteen days study. For fifteen days study, blood samples were taken from rats at 0, 7 and 15 days. The data obtained (Table 7) showed also all compounds had significant hypoglycemic effect upon comparison to rosiglitazone. Compounds showed higher inhibitory activities against α-glucosidase and β-glucosidase (**12e**, **12f**, **13b** and **13c**) showed considerable hypoglycemic effect relative to rosiglitazone; at 7th day, the blood glucose levels were 191.58, 150.08, 210.49 and 214.59 mg/dl respectively relative to rosiglitazone = 120.07. At 15th day, the blood glucose levels were 140.38, 128.96, 212.57 and 171.49 mg/dl respectively relative to rosiglitazone = 104.06.

2.3. Molecular modeling

2.3.1. Shape alignment and scoring using ROCS

Rapid Overlay of Chemical Structures (ROCS) is used to perceive similarity between molecules based on their three dimensional shape [46]. Shape similarity is considered as a fundamental descriptor for computational drug discovery to model and understand correctly about the protein ligand interactions [47]. Shape exhibits good neighborhood behaviors that high similarity in shape behaves reflective of high similarity in biology and not by any means similar in 2D [48]. ROCS alignment requires query molecules (celecoxib and rosiglitazone) and database molecules (the target compounds thiazolidindione s **12a-f** and thiazolidinones **13a-f**). The quality of alignment between database and query was calculated using Tanimoto Combo score which is the summation of Shape Tanimoto and Color Tanimoto [46]. Shape Tanimoto represents the shared volume and mismatch volume and has a scale from 0 to 1.0 while Color Tanimoto is reflective for the degree of matching or mismatching of light chemical features in 3 dimensions

Table 7
Hypoglycemic activity of the target compounds (**12a-f** and **13a-f**) and reference drug rosiglitazone (fifteen days study).

Compound	0 h	7th day	15th day
12a	307.29 ± 4.015	230.96 ± 0.763****	175.77 ± 0.517****
12b	276.52 ± 0.868	211.65 ± 1.844****	150.636 ± 0.174****
12c	280.42 ± 0.241	219.083 ± 1.366****	154.746 ± 1.002****
12d	270.59 ± 0.3080	212.356 ± 2.870****	161.533 ± 1.104****
12e	254.326 ± 1.275	191.576 ± 1.701****	140.376 ± 1.544****
12f	231.81 ± 0.622	150.08 ± 0.710****	128.956 ± 2.907****
13a	321.59 ± 0.895	211.865 ± 1.106	206.44 ± 1.307
13b	279.263 ± 1.510	210.493 ± 1.129****	212.566 ± 0.985****
13c	261.45 ± 1.005	214.586 ± 1.126****	171.486 ± 1.063****
13d	254.143 ± 1.276	216.696 ± 1.3090****	141.856 ± 2.393****
13e	311.026 ± 0.449	251.39 ± 0.783****	182.236 ± 1.703****
13f	281.95 ± 1.172	221.57 ± 1.153****	180.556 ± 0.7715****
Diabeticcontrol	319.446 ± 0.185	320.586 ± 0.635	319.446 ± 1.058
Rosiglitazone	308.956 ± 0.517	120.073 ± 0.519****	104.06 ± 0.274****

Values represent means ± SEM of four animals for each group.
**** Means significant difference with reference drug at $p < 0.01$.

Table 8
Tanimoto Combo (TC) score of the target derivatives (**12a-f** and **13a-f**) in comparison to celecoxib and rosiglitazone.

Compound	TC in comparison with celecoxib	TC in comparison with rosiglatazone
12a	0.93	0.77
12b	0.97	0.75
12c	0.95	0.74
12d	1.1	0.69
12e	0.95	0.64
12f	0.99	0.72
13a	1.0	0.75
13b	0.95	0.77
13c	0.69	0.69
13d	0.93	0.71
13e	0.64	0.48
13f	0.9	0.73

and also has a scale from 0 to 1.0. Both query and database molecules are combined into a single species using fragment disconnected non-chemically meaning pieces of a molecule [46]. The Tanimoto Combo scores for all target compounds thiazolidindione s **12a-f** and thiazolidinones **13a-f** are listed in Table 8. The data revealed that the TC scores for thiazolidindione s **12a-f** (0.93–1.10) which are significantly higher than TC scores for thiazolidinones **13a-f** (0.64–1.00) upon alignment with celecoxib query. On the contrary, upon alignment with rosiglitazone query, the TC scores for thiazolidindione s **12a-f** and thiazolidinones **13a-f** are approximately close to each other (0.64–0.77 and 0.48–0.77 respectively) and they were lower than the TC scores obtained upon alignment with celecoxib.

ROCS shape and color analyses for celecoxib as query model showed Y shape volume with 2 acceptors, 2 donors and 3 rings (Fig. 4a) while rosiglitazone adopted as boat shape with 3 acceptors, 1 donor and 3 rings species (Fig. 4b). The alignment and overly lay using ROCS between celecoxib (query) and database molecules (thiazolidindione s **12a-f** and thiazolidines **13a-f**) showed that **12a-f** aligned completely with celecoxib shape (Fig. 5a) while **13a-f** exhibited alignment as the thiazolidine arm locates outside the query shape (Fig. 5b). Interestingly the thiazolidinone derivative **13c** (The most potent COX-2 inhibitor with IC_{50} = 0.61 μM) had its own overly with the celecoxib shape rather than the other analogues (**13a**, **13b**, **13d**, **13e** and **13f**) (Fig. 5c).

On the other hand, **12a-f** (Fig. 6a) and **13a-f** (Fig. 6b) aligned and overlaid completely within the rosiglitazone shape with a difference in the position of aryl part which was located outside query volume. Compound **12f** (the higher thiazolidindione derivative in induction of PPAR-γ activation 59.63%) occupied the rosiglitazone volume and its thiazolidine part was located on the same volume of rosiglitazone thiazolidine ring (Fig. 6c).

2.3.2. Molecular docking study

Our intention was directed to examine the activity and selectivity of the target compounds (thiazolidindione s **12a-f** and thiazolidines **13a-f**) based on their docking pose and mode with COX-2 and PPARγ enzymes. For docking against COX-2, a library of **12a-f**, **13a-f** and celecoxib as a reference COX-2 selective drug was energy minimized using MMFF94 force field calculations. The catalytic domain of COX-2 (PDB code: 3LN1) [49] was prepared for docking using Open Eye® software [50–52]. To validate our docking procedure, celecoxib was docked with COX-2 (PDB: ID 3LN1) and showed binding mode and pose similar to its co-crystallized [49]. It was clear that the thiazolidindione series **12a-f** (with methylene linker) exhibited the same pose and mode as celecoxib while the thiazolidinone series **13a-f** (with methylenehydrazone linker) exhibited different pose since the methylenehydrazone thiazolidine part was located in lower motif of the receptor as shown in Figs. 7 and 8. Both compounds **12a** (the most potent COX-2 inhibitor in this study with IC_{50} = 0.48 μM) and **12c** (high COX-2 activity and selectivity (IC_{50} = 0.63 μM, SI = 9.15) overlay each other in the catalytic domain with same pose. compound **12c** interacts with the active site through hydrogen bond (HB) through its methylsulfonyl group with PHE 504 AA and by it backbone through hydrophobic-hydrophobic interactions (Fig. 7a). Both celecoxib and compound **12c** overlay each other with indication for keeping the pharmacophore similarity of both compounds that both form the similar Y shape (Fig. 7b). Compound **13f**, the most COX-2 selective derivative in the thiazolidinone series **13a-f**, with COX-2 IC_{50} = 0.62 μM and SI = 9.15 docked with the receptor without formation of HB and only formed hydrophobic-hydrophobic interaction with different pose (Fig. 8).

Regarding docking with PPARγ receptor, The most potent derivatives **12e**, **12f**, **13b** and **13c** were chosen to analyze their interaction with PPARγ (ID: 4O8F) [53] and to compare their binding pattern to the co-crystal ligand. Rosiglitazone as a ligand docked similar to it co-crystallized pose with formation of HB with Arg 288 AA and Ser 289 AA

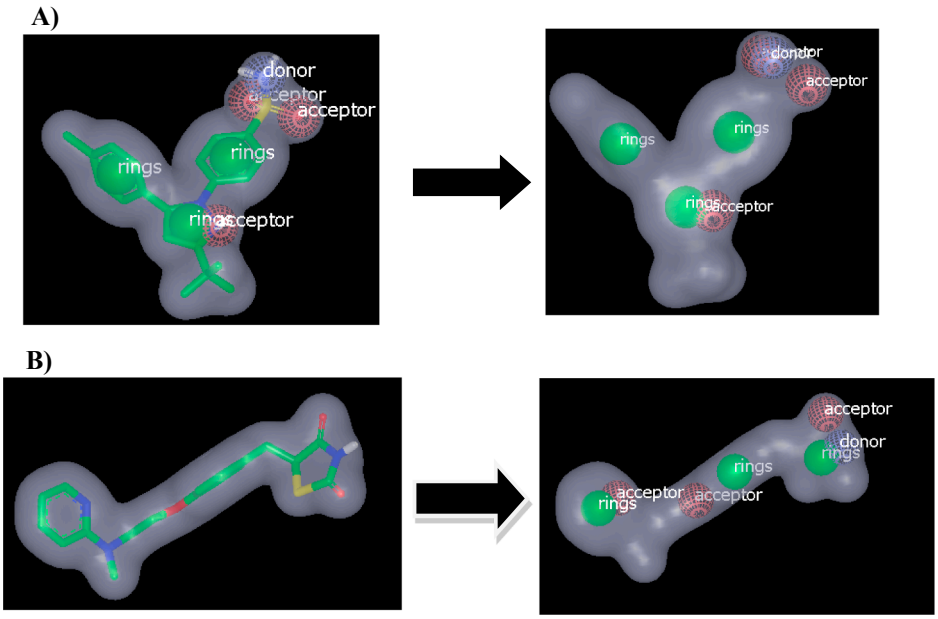

Fig. 4. (A) Representation shape and color atoms of celecoxib by vROCS application; (B) representation shape and color atoms of rosiglitazone vROCS application.

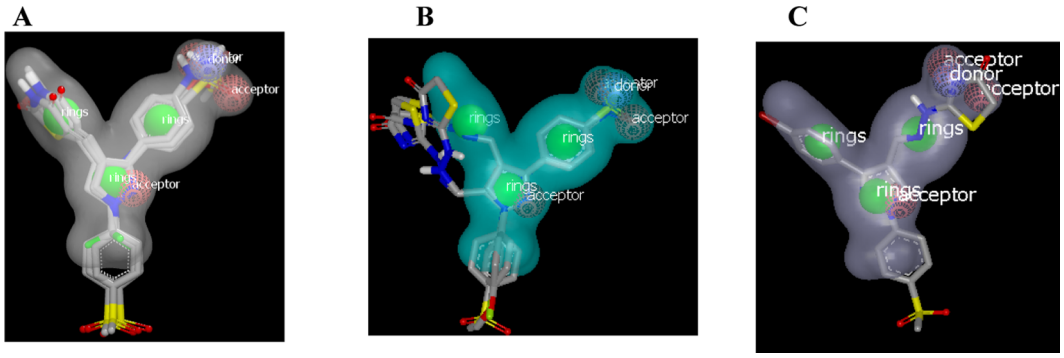

Fig. 5. (A) Overlay and alignment of thiazolidindione s **12a-f** on celecoxib shape; (B) overlay and alignment of thiazolidinones **13a-f** on celecoxib shape; (C) compound **13c** exhibited specific shape alignment with celecoxib.

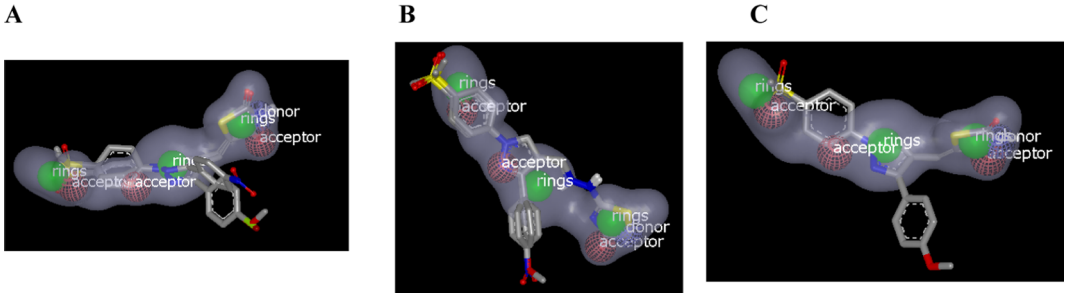

Fig. 6. (A) Overlay and alignment of thiazolidindione s **12a-f** on rosiglitazone shape; (B) overlay and alignment of thiazolidinones **13a-f** on rosiglitazone shape; (C) compound **12f** exhibited specific shape alignment with celecoxib.

while compound **12f** docked similarly by formation of two HB with Arg 288 AA through the N of pyrazole moiety (as acceptor) and one HB as acceptor with Ser 289 AA through the carbonyl of thiazolidindione ring in addition to one HB as donor with Tyr 327 through the NH of thiazolidindione, and hydrophobic-hydrophobic interaction with remain backbone of compound **12f**. Also, the *P*-methoxy phenyl part of **12f** occupied the pocket to form as axial part of **Y** shape (Fig. 9a). The other thiazolidindione derivative **12e** and the most PPARγ activator (**13b**, 63.15%), both overlay together (Fig. 9b), adopted the same pose and mode (Y shape pose in side left motif of active site) through hydrophobic-hydrophobic interactions only in different pocket from standard rosiglitazone which is the same domain as pioglitazone occupied [54]. Briefly, the analyzed compounds **12e**, **12f**, **13b** and **13c** successfully adopted the Y shape (Fig. 9c) which is essential for activity and two of them **12f** and **13c** docked with PPARγ at the same area of rosiglitazone while the other two **12e** and **13b** interacted with the receptor in the left motif as pioglitazone.

3. Conclusion

Two new series of thiazolidine derivatives containing pyrazole core **12a-f** and **13a-f** were synthesized as hybrid structures to be evaluated for their COX inhibitory activity, anti-inflammatory activity ulcerogenic liability, *α*- and *β*-glucosidase inhibition activity, PPAR-γ assay and the *in vivo* anti-diabetic evaluation. Structure-activity data acquired and biological studies revealed that (i) all compounds were more COX-2 inhibitors than COX-1 and four of them (**12c**, **12f**, **13b** and **13f**) had higher COX-2 S.I. (8.69–9.26) than the COX-2 selective drug celecoxib (COX-2 S.I. = 8.60), (ii) The most COX-2 selective derivatives **12c**, **12f**, **13b** and **13f** showed the highest AI activities and the lowest ulcerogenicity than other derivatives, (iii) two thiazolidindione derivatives **12e** and **12f** and two thiazolidinone derivatives **13b** and **13c** showed higher inhibitory activities against *α*- and *β*-glucosidase (% inhibitory activity = 62.15, 55.30, 65.37, 59.08 for α-glucosidase and 57.42, 60.07, 58.19, 66.90 for β-glucosidase respectively) than reference

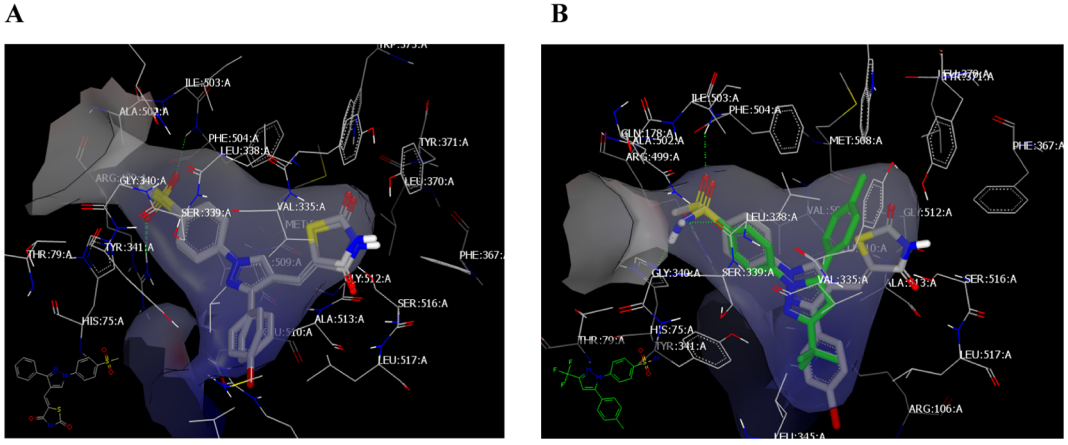

Fig. 7. (A) **12a** and **12c** in catalytic domain of COX-2 (PDB code: 3LN1); (B) **12c** and celecoxib in catalytic domain of COX-2 (PDB code: 3LN1).

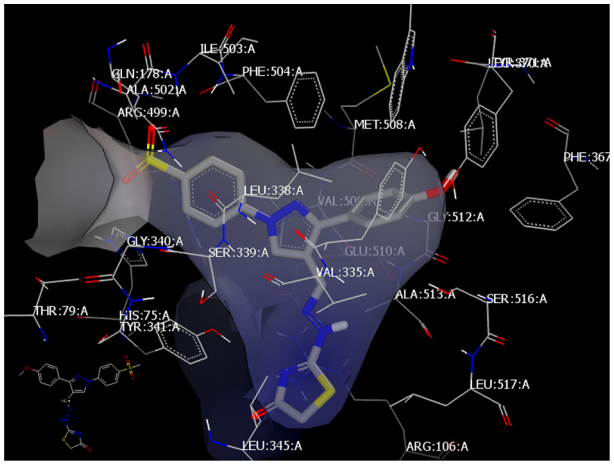

Fig. 8. 13f in catalytic domain of COX-2 (PDB code: 3LN1).

compounds (acarbose and D-Saccharic acid 1,4-lactone monohydrate), (iv) The four derivatives **12e**, **12f**, **13b** and **13c** showed good PPAR-γ activation and good hypoglycemic effect in comparison to pioglitazone and rosiglitazone, (v) The difference in spacer between 2 series; thiazolidindione series **12a-f** (methylene spacer) and thiazolidinone series **13a-f** (methylenehydrazone spacer) affects the binding of the derivatives with the receptor and finally (vi) We can conclude that the combination of pharmacophoric moieties of different bioactive substances in one hybrid structure can be used as an efficient strategy for the synthesis of compounds with dual biological activities.

4. Experimental section

4.1. Chemistry

General: Melting points were determined on a Thomas-Hoover capillary apparatus and are uncorrected. Infrared (IR) spectra were recorded as films on KBr plates using a Nicolet 550 Series II Magna FT-IR spectrometer. ^{1}H NMR and ^{13}C NMR spectra were measured on a Bruker 400 MHz NMR Spectrophotometer, Faculty of Pharmacy, Beni-Suef University, Egypt in $CDCl_3$ or DMSO-d_6 with TMS as the internal standard, where *J* (coupling constant) values are estimated in Hertz (Hz). Mass spectra (MS) were recorded on a Water's Micromass ZQ 4000 mass spectrometer using the electro-spray (ES) ionization mode. Microanalyses were performed for C, H and N were carried out on Perkin-Elmer 2400 analyzer (Perkin-Elmer, Norwalk, CT, USA) at the Microanalytical unit of Cairo University, Egypt. All compounds were within ± 0.4% of the theoretical values. Silica gel column chromatography was performed using Merck silica gel 60 ASTM (70–230 mesh). Compounds **8b-d**, **9b-d** [39] and **11** [11] were prepared according to the previously reported procedures.

4.1.1. General procedure for synthesis of hydrazones (*8a, 8e and 8f*)

To a solution of the appropriate acetophenone (0.04 mol) in 20 mL ethanol, 4-methanesulfonyl phenyl hydrazine hydrochloride (**6a**, 0.04 mol) was added. The resulting solution was heated under reflux for 12 h. The precipitated hydrazones was filtered and washed with sufficient amount of ethanol and recrystallized from ethanol to afford hydrazones **8a**, **8b** and **8f**. Physical and spectral data are listed below:

*4.1.1.1. (E)-1-(4-(methylsulfonyl)phenyl)-2-(1-phenylethylidene) hydrazine (**8a**).* Yield 77%; white solid; m.p. 218–220 °C; IR (KBr): 3319 (NH), 3020 (C—H aromatic), 2923 (C—H aliphatic), 1598 (C═N), 1327, 1138, (SO_2CH_3) cm^1; ^{1}H NMR (DMSO-d_6, 400 MHz, *δ*, ppm): 2.32 (s, 3H, $\underline{CH_3}$—C═N), 3.11 (s, 3H, $SO_2\underline{CH_3}$),7.33 (m, 3H, phenyl H-3, H-4, H-5), 7.42 (d, 2H, *J* = 7.8 Hz, phenyl H-2, H-6), 7.73 (d, 2H, *J* = 8.4 Hz methanesulfonylphenyl H-3, H-5), 7.82 (d, 2H, *J* = 8.4 Hz, methanesulfonylphenyl H-2, H-6), 9.90 (s, 1H, -NH-, D_2O Exchangeable); MS *m/z* (ES^+) 288 (M^+) (25%); Anal. Calcd. For $C_{15}H_{16}N_2O_2S$; C, 62.48; H, 5.59; N, 9.71; Found; C, 62.63; H, 5.83; N, 9.81.

*4.1.1.2. (E)-N-(4-(1-(2-(4-(methylsulfonyl)phenyl)hydrazono)ethyl) phenyl)methanesulfonamide (**8e**).* Yield 66%; white solid; m.p. 208–210 °C; IR (KBr): 3424 ($\underline{NH}SO_2CH_3$) 3295 ($\underline{NH}$—N═C), 3022 (C—H aromatic), 2930 (C—H aliphatic), 1594 (C═N), 1373, 1151, (SO_2CH_3) cm^1; ^{1}H NMR (DMSO-d_6, 400 MHz, *δ*, ppm): 2.35 (s, 3H, $\underline{CH_3}$—C═N), 3.12 (s, 3H, $SO_2\underline{CH_3}$), 3.22 (s, 1H, $\underline{NH}SO_2CH_3$, D_2O exchangeable), 3.55 (s, 3H, $NHSO_2\underline{CH_3}$), 7.41 (d, 2H, *J* = 7.6 Hz methanesulfonylphenyl H-2, H-6), 7.53 (d, 2H, *J* = 8.4 Hz, *N*-phenylmethanesulfonamide H-3, H-5), 7.75 (d, 2H, *J* = 7.6 Hz methanesulfonylphenyl H-3, H-5), 7.89 (d, 2H, *J* = 8.4 Hz, *N*-phenylmethanesulfonamide H-2, H-6), 10.04 (s, 1H, NH, D_2O exchangeable); MS *m/z* (ES^+) 381 (M^+) (62%). Anal. Calcd. For $C_{16}H_{19}N_3O_4S_2$; C, 50.38; H, 5.02; N, 11.02; Found; C, 50.35; H, 5.24; N, 10.89

*4.1.1.3. (E)-1-(1-(4-methoxyphenyl)ethylidene)-2-(4-(methylsulfonyl) phenyl)hydrazine (**8f**).* Yield 81%; white solid; m.p. 236–238 °C; IR (KBr): 3308 (NH), 3011 (C—H aromatic), 2968 (C—H aliphatic), 1594 (C═N), 1343, 1130, (SO_2CH_3) cm^1; ^{1}H NMR (DMSO-d_6, 400 MHz, *δ*, ppm): 2.28 (s, 3H, $\underline{CH_3}$—C═N), 3.11 (s, 3H, $SO_2\underline{CH_3}$), 3.78 (s, 3H, $O\underline{CH_3}$), 6.96 (d, 2H, *J* = 8.2 Hz, 4-methoxyphenyl H-3, H-5), 7.35 (d, 2H, *J* = 8.2 Hz, 4-methoxyphenyl H-2, H-6), 7.71 (d, 2H, *J* = 8.4 Hz methanesulfonylphenyl H-3, H-5), 7.76 (d, 2H, *J* = 8.2 Hz, methanesulfonylphenyl H-2, H-6), 9.81 (s, 1H, NH, D_2O exchangeable); MS *m/z* (ES^+) 318 (M^+) (38%). Anal. Calcd. for:

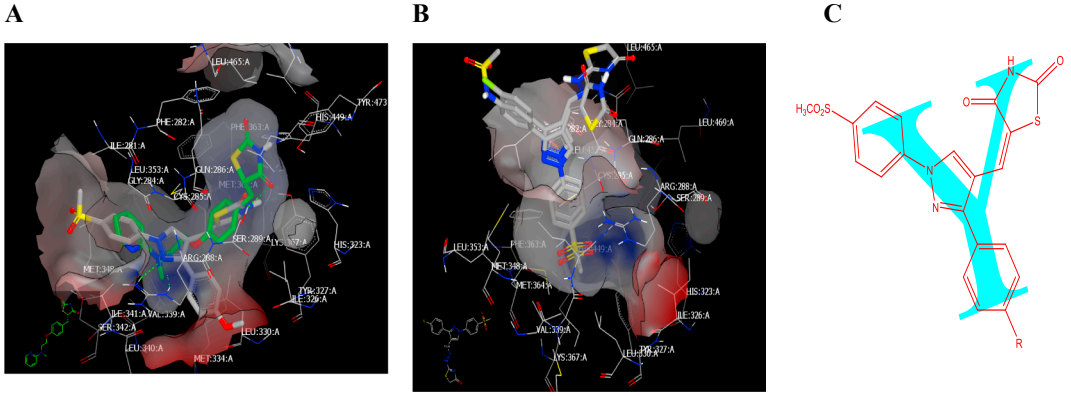

Fig. 9. (A) **12f** and rosiglitazone in domain of PPARγ (PDB code: 408F); (B) **12e** and **13b** in domain of PPARγ (PDB code: 408F); (C) Y shaped adopted by tested compounds inside PPARγ receptor.

$C_{16}H_{18}N_2O_3S$; C, 60.36; H, 5.70; N, 8.80; Found; C, 60.19; H, 5.64; N, 8.55

*4.1.2. General procedure for synthesis of 3-aryl-1-phenyl-1H-pyrazole-4-carbaldehyde (**9a, 9e** and **9f**)*

To a cold solution of dimethylformamide (30 mL) and phosphorous oxychloride (83.58 mmol) hydrazone (**8a**, **8e** or **8f**, 20.24 mmol) was added. The reaction mixture was stirred at 55–60 °C for 12 h, cooled to room temperature, poured into ice cold water and neutralized with saturated aqueous sodium bicarbonate solution whereupon a solid separated out was filtered, washed with excess of cold water, dried and crystalized from ethanol to afford aldehydes **9a**, **9e** and **9f**. Physical and spectral data are listed below:

*4.1.2.1. 1-(4-(methylsulfonyl)phenyl)-3-phenyl-1H-pyrazole-4-carbaldehyde (**9a**)*. Yield 56%; pale yellow solid; m.p. 178–180 °C IR (KBr: 3122 (C—H aromatic), 2979 (C—H aliphatic), 1675 (C=O), 1528 (C=N), 1369, 1144, (SO_2CH_3) cm^{-1}; ^1H NMR (DMSO-d_6, 400 MHz, δ, ppm): 3.27 (s, 3H, $SO_2\underline{CH_3}$), 7.53 (m, 3H, phenyl H-3, H-4, H-5), 7.95 (d, 2H, J = 8.4 Hz, phenyl H-2, H-6), 8.14 (d, 2H, J = 8.4 Hz, methanesulfonylphenyl H-3, H-5), 8.29 (d, 2H, J = 8.4 Hz, methanesulfonylphenyl H-2, H-6), 9.50 (s, 1H, pyrazole H-5), 10.02 (s, 1H, CHO); MS m/z (ES^+) 326 (M^+) (66%). Anal. Calcd. For $C_{17}H_{14}N_2O_3S$, C, 62.56, H, 4.32, N, 8.58; Found; C, 62.39; H, 4.37; N, 8.32.

*4.1.2.2. N-(4-(4-formyl-1-(4-(methylsulfonyl)phenyl)-1H-pyrazol-3-yl) phenyl)methanesulfonamide (**9e**)*. Yield 46%; pale yellow solid; m.p. 197–199 °C IR (KBr: 3110 (C—H aromatic), 2934 (C—H aliphatic), 1693 (C=O), 1519 (C=N), 1346, 1151, (SO_2CH_3) cm^{-1}; ^1H NMR (DMSO-d_6, 400 MHz, δ, ppm): 3.12 (s, 3H, $SO_2\underline{CH_3}$), 3.22 (s, 1H, $\underline{NH}SO_2CH_3$, D_2O exchangeable), 3.55 (s, 3H, $NHSO_2\underline{CH_3}$), 8.07 (d, 2H, J = 7.6 Hz methanesulfonylphenyl H-2, H-6), 8.10 (d, 2H, J = 8.4 Hz, *N*-phenylmethanesulfonamide H-3, H-5), 8.26 (d, 2H, J = 7.6 Hz methanesulfonylphenyl H-3, H-5), 8.29 (d, 2H, J = 8.4 Hz, *N*-phenylmethanesulfonamide H-2, H-6), 9.49 (s, 1H, pyrazole H-5), 10.00 (s, 1H, CHO); MS m/z (ES^+) 419 (M^+) (100%). Anal. Calcd. For $C_{18}H_{17}N_3O_5S_2$: C, 51.54; H, 4.08; N, 10.02; Found; C, 51.64; H, 4.04; N, 9.85.

*4.1.2.3. 3-(4-methoxyphenyl)-1-(4-(methylsulfonyl)phenyl)-1H-pyrazole-4-carbaldehyde (**9f**)*. Yield 55%; pale yellow solid; m.p. 185–187 °C IR (KBr: 3064 (C—H aromatic), 2952 (C—H aliphatic), 1678 (C=O), 1521 (C=N), 1294, 1146, (SO_2CH_3) cm^{-1}; ^1H NMR (DMSO-d_6, 400 MHz, δ, ppm): 3.31 (s, 3H, $SO_2\underline{CH_3}$), 3.83 (s, 3H, $O\underline{CH_3}$), 7.61 (d, 2H, J = 8.4 Hz, methoxyphenyl H-3, H-5), 7.78 (d, 2H, J = 8.4 Hz, methoxyphenyl H-2, H-6), 7.91 (d, 2H, J = 8.4 Hz, methanesulfonylphenyl H-3, H-5), 8.10 (d, 2H, J = 8.4 Hz, methanesulfonylphenyl H-2, H-6), 9.49 (s, 1H, pyrazole H-5), 10.00 (s, 1H, CHO); MS m/z (ES^+) 3.56 (M^+) (100%). Anal. Calcd. For $C_{18}H_{16}N_2O_4S$: C, 60.66, H, 4.53, N, 7.86; Found; C, 60.78; H, 4.13; N, 7.66.

*4.1.3. General procedure for synthesis of the (Z)-2-((1-(4-(methylsulfonyl) phenyl)-3-substituted-1H-pyrazol-4-yl)methylene)hydrazinecarbothioamide (**10a-f**)*

To a hot solution of the appropriate pyrazole aldehyde (**9a-f**) (2 mmol) in absolute ethanol (20 mL), thiosemicarbazide (2.0 mmol) was added. The reaction mixture was heated under reflux for 24 h, the formed precipitated was filtered and recrystallized from ethanol. Physical and spectral data are listed below:

*4.1.3.1. (Z)-2-((1-(4-(methylsulfonyl)phenyl)-3-phenyl-1H-pyrazol-4-yl) methylene)-hydrazinecarbothioamide (**10a**)*. Yield 72%; white solid; mp 195–197 °C; IR (KBr): 3461–3335 (NH_2), 3132 (NH), 3005 (C—H aromatic), 2923 (C—H aliphatic), 1594 (C=N), 1505 (C=S), 1373, 1146 (SO_2CH_3) cm^{-1}; ^1H NMR (DMSO-d_6, 400 MHz, δ, ppm): 3.30 (s, 3H, $SO_2\underline{CH_3}$), 7.53 (m, 3H, phenyl H-3, H-4, H-5), 7.71(d, 2H, J = 8.4 Hz, phenyl H-2, H-6), 7.81 (s, 2H, NH_2, D_2O exchangeable), 8.00 (d, 2H, J = 8.0 Hz, methanesulfonylphenyl H-3, H-5), 8.16 (d, 2H, J = 8.0 Hz, methanesulfonylphenyl H-2, H-6), 8.31 (s, 1H, olefinic C—H), 9.34 (s, 1H, pyrazole H-5), 11.39 (s, 1H, NH, D_2O exchangeable); ^{13}C NMR (DMSO- d_6 100 MHz, δ, ppm): 44.12, 118.76, 119.11, 128.69, 128.80, 129.27, 129.39, 129.44, 132.15, 134.95, 138.97, 142.83, 152.79, 178.20; MS m/z (ES^+) 399 (M+) (100%). Anal. Calcd. For $C_{18}H_{17}N_5O_2S_2$: C, 54.12; H, 4.29; N, 17.53; Found; C, 54.76; H, 4.39; N, 17.79.

*4.1.3.2. (Z)-2-((3-(4-chlorophenyl)-1-(4-(methylsulfonyl)phenyl)-1H-pyrazol-4-yl)methylene)-hydrazinecarbothioamide (**10b**)*. Yield 55%; white solid; mp 210–212 °C; IR (KBr): 3419–3333 (NH_2), 3153 (NH), 3005 (C—H aromatic), 2923 (C—H aliphatic), 1594 (C=N), 1504 (C=S), 1339, 1148 (SO_2CH_3) cm^{-1}; ^1H NMR (DMSO-d_6, 400 MHz, δ, ppm): 3.29 (s, 3H, $SO_2\underline{CH_3}$), 7.68 (m, 6H, methanesulfonylphenyl H-3, H-5, H-2, H-6 and 2H, NH_2, D_2O exchangeable), 8.15 (d, 2H, J = 8.4 Hz, 4-chlorophenyl H-2, H-6), 8.19 (d, 2H, J = 8.0 Hz, 4-chlorophenyl H-3, H-5), 8.33 (s, 1H, olefinic C—H), 9.35 (s, 1H, pyrazole H-5), 11.38 (s, 1H, NH, D_2O exchangeable); ^{13}C NMR (DMSO- d_6 100 MHz, δ, ppm): 44.02, 118.76, 119.20, 122.86, 129.01, 129.45, 130.65, 131.33, 132.26, 134.69, 139.07, 142.72, 151.59, 178.15; MS m/z (ES^+) 433 (M+) (68%). Anal. Calcd. For $C_{18}H_{16}ClN_5O_2S_2$: C, 49.82; H, 3.72; N, 16.14; Found; C, 49.76; H, 3.39; N, 16.19.

*4.1.3.3. (Z)-2-((3-(4-bromophenyl)-1-(4-(methylsulfonyl)phenyl)-1H-pyrazol-4-yl)methylene)-hydrazinecarbothioamide (**10c**)*. Yield 77%; white solid; mp 182–184 °C; IR (KBr): 3404–3275 (NH_2), 3138 (NH), 3003 (C—H aromatic), 2921 (C—H aliphatic), 1598 (C=N), 1505 (C=S), 1370, 1145 (SO_2CH_3) cm^{-1}; ^1H NMR (DMSO-d_6, 400 MHz, δ, ppm): 3.29 (s, 3H, $SO_2\underline{CH_3}$), 6.47 (s, 2H, NH_2, D_2O exchangeable), 7.64 (d, 2H, J = 8.4 Hz, methanesulfonylphenyl H-2, H-6), 7.71 (d, 2H, J = 8.4 Hz, 4-bromophenyl H-2, H-6), 7.94 (s, 1H, olefinic C—H), 8.09 (d, 2H, J = 8.4 Hz, methanesulfonylphenyl H-3, H-5), 8.16 (d, 2H, J = 8.4 Hz, 4-bromophenyl H-3, H-5), 9.24 (s, 1H, pyrazole H-5), 10.18 (s, 1H, NH, D_2O exchangeable); ^{13}C NMR (DMSO- d_6 100 MHz, δ, ppm): 40.13, 105.58, 115.58, 119.05, 128.20, 129.98, 132.17, 132.82, 138.52, 139.07, 141.90, 142.35, 142.91, 163.85; MS m/z (ES^+) 476 (M+) (100%). Anal. Calcd. For $C_{18}H_{16}BrN_5O_2S_2$: C, 45.19; H, 3.37; N, 14.64; Found; C, 45.55; H, 3.39; N, 14.79.

*4.1.3.4. (Z)-2-((1-(4-(methylsulfonyl)phenyl)-3-(4-nitrophenyl)-1H-pyrazol-4-yl)methylene-)hydrazinecarbothioamide (**10d**)*. Yield 77%; white solid; mp 220–222 °C; IR (KBr): 3461–3335 (NH_2), 3118 (NH), 3004 (C—H aromatic), 2925 (C—H aliphatic), 1595 (C=N), 1518 (C=S), 1343, 1149 (SO_2CH_3) cm^{-1}; ^1H NMR (DMSO-d_6, 400 MHz, δ, ppm): 3.30 (s, 3H, $SO_2\underline{CH_3}$), 7.76 (s, 2H, NH_2, D_2O exchangeable), 7.81 (d, 2H, J = 8.0 Hz, methanesulfonylphenyl H-2, H-6), 8.00 (d, 2H, J = 7.6 Hz, 4-nitrophenyl H-2, H-6), 8.13 (d, 2H, J = 8.0 Hz, methanesulfonylphenyl H-3, H-5), 8.18 (s, 1H, olefinic C—H), 8.25 (d, 2H, J = 8.4 Hz, 4-bromophenyl H-3, H-5), 9.39 (s, 1H, pyrazole H-5), 11.42 (s, 1H, NH, D_2O exchangeable); ^{13}C NMR (DMSO- d_6 100 MHz, δ, ppm): 44.03, 105.58, 119.39, 124.43, 129.47, 129.71, 134.31, 138.56, 139.38, 142.58, 147.88, 150.39, 155.91, 178.23; MS m/z (ES^+) 444 (M+) (100%). Anal. Calcd. For $C_{18}H_{16}N_6O_4S_2$: C, 48.64; H, 3.63; N, 18.91; Found; C, 48.76; H, 3.39; N, 18.79.

*4.1.3.5. (Z)-2-((3-(4-(methylsulfonamido)phenyl)-1-(4-(methylsulfonyl) phenyl)-1H-pyrazol-4-yl)methylene)hydrazinecarbothioamide (**10e**)*. Yield 61%; white solid; mp 188–190 °C; IR (KBr): 3455–3358 (NH_2), 3152 (NH), 3011 (C—H aromatic), 2926 (C—H aliphatic), 1595 (C=N), 1504 (C=S), 1371, 1152 (SO_2CH_3) cm^{-1}; ^1H NMR (DMSO-d_6, 400 MHz, δ, ppm): 3.30 (s, 3H, $SO_2\underline{CH_3}$), 3.22 (s, 1H, $\underline{NH}SO_2CH_3$, D_2O exchangeable), 3.31 (s, 3H, $NHSO_2\underline{CH_3}$), 7.69 (d, 2H, J = 7.6 Hz methanesulfonylphenyl H-2, H-6), 7.71 (s, 2H, NH_2, D_2O

exchangeable), 8.13 (d, 2H, J = 7.6 Hz, *N*-phenylmethanesulfonamide H-3, H-5), 8.26 (d, 2H, J = 7.6 Hz methanesulfonylphenyl H-3, H-5), 8.18 (s, 1H, olefinic C—H), 8.26 (d, 2H, J = 8.4 Hz, *N*-phenylmethanesulfonamide H-2, H-6), 9.38 (s, 1H, pyrazole H-5), 11.39 (s, 1H, NH, D_2O exchangeable); ^{13}C NMR (DMSO- d_6 100 MHz, δ, ppm): 43.59, 44.05, 119.23, 119.82, 128.99, 129.47, 129.67, 131.94, 133.88, 134.59, 134.76, 139.19, 142.74, 151.57, 178.22; MS *m/z* (ES^+) 399 (M +) (100%). Anal. Calcd. For $C_{19}H_{20}N_6O_4S_3$: C, 46.33; H, 4.09; N, 17.06; Found; C, 46.76; H, 4.39; N, 17.29.

*4.1.3.6. (Z)-2-((3-(4-methoxyphenyl)-1-(4-(methylsulfonyl)phenyl)-1H-pyrazol-4-yl)methylene)-hydrazinecarbothioamide (**10f**)*. Yield 81%; white solid; mp 224–226 °C; IR (KBr): 3367–32577 (NH_2), 3123 (NH), 3004 (C—H aromatic), 2966 (C—H aliphatic), 1594 (C═N), 1523 (C═S), 1403, 1148 (SO_2CH_3) cm^1; ^{1}H NMR (DMSO-d_6, 400 MHz, δ, ppm): 3.30 (s, 3H, $SO_2\underline{CH_3}$), 3.88 (s, 3H, $O\underline{CH_3}$), 7.08 (d, 2H, J = 8.0 Hz, 4-methoxyphenyl H-2, H-6), 7.63 (d, 2H, J = 8.0 Hz, 4-methoxyphenyl H-3, H-5), 7.76 (s, 2H, NH_2, D_2O exchangeable), 8.10 (d, 2H, J = 8.0 Hz, methanesulfonylphenyl H-2, H-6), 8.21 (d, 2H, J = 8.0 Hz, methanesulfonylphenyl H-3, H-5), 8.29 (s, 1H, olefinic C—H), 9.30 (s, 1H, pyrazole H-5), 11.37 (s, 1H, NH, D_2O exchangeable); ^{13}C NMR (DMSO- d_6 100 MHz, δ, ppm): 44.08, 55.78, 106.66, 114.71, 118.61, 118.98, 124.50, 127.55, 130.02, 135.12, 138.79, 142.85, 152.64, 160.29, 178.12; MS *m/z* (ES^+) 429 (M +) (100%). Anal. Calcd. For $C_{19}H_{19}N_5O_3S_2$: C, 53.13; H, 4.46; N, 16.31; Found; C, 55.29; H, 4.39; N, 16.55.

*4.1.4. General procedure for synthesis of the thiazolidindione derivatives (**12a-f**)*

To a hot solution of the appropriate pyrazole aldehydes (**9a-f**) (2 mmol) in absolute ethanol (20 mL), thiazolidine-2,4-dione (**11**, 2.0 mmol) was added with few drops of pipridine. The reaction mixture was heated under reflux for 24 h, the formed precipitate was filtered and recrystallized from ethanol to give the final derivatives (**12a-f**). Physical and spectral data are listed below:

*4.1.4.1. (E)-5-((1-(4-(methylsulfonyl)phenyl)-3-phenyl-1H-pyrazol-4-yl) methylene)thiazolidine-2,4-dione (**12a**)*. Yield 33%; yellow solid; m.p. 125–127 °C; IR (KBr): 3219 (NH), 3117 (C—H aromatic), 2923 (C—H aliphatic), 1755, 1707 (C═O), 1615 (—CH═C—), 1594 (C═N), 1325, 1138 (SO_2CH_3) cm^1; ^{1}H NMR (DMSO-d_6, 400 MHz, δ, ppm): 3.30 (s, 3H, $SO_2\underline{CH_3}$), 7.55 (m, 3H, phenyl H-3, H-4, H-5), 7.57 (d, 2H, J = 7.6 Hz, phenyl H-2, H-6), 7.56 (s, 1H, olefinic C—H), 8.09 (d, 2H, J = 7.6 Hz, methanesulfonylphenyl H-3, H-5), 8.31 (d, 2H, J = 7.6 Hz, methanesulfonylphenyl H-2, H-6), 8.84 (s, 1H, pyrazole H-5), 12.33 (s, 1H, NH, D_2O exchangeable); ^{13}C NMR (DMSO- d_6 100 MHz, δ, ppm): 44.76, 115.82, 122.00, 122.93, 127.33, 128.12, 128.96, 129.18, 129.30, 129.48, 129.73, 131.74, 133.02, 141.25, 167.30, 167.85; MS *m/z* (ES^+) 425 (M +) (100%). Anal. Calcd. For $C_{20}H_{15}N_3O_4S_2$: C, 56.46; H, 3.55; N, 9.88; Found; C, 56.76; H, 3.39; N, 9.79.

*4.1.4.2. (E)-5-((3-(4-chlorophenyl)-1-(4-(methylsulfonyl)phenyl)-1H-pyrazol-4-yl)methylene)-thiazolidine-2,4-dione (**12b**)*. Yield 33%; yellow solid; m.p. 156–158 °C; IR (KBr): 3117 (NH), 3017 (C—H aromatic), 2955 (C—H aliphatic), 1745, 1701 (C═O), 1615 (—CH═C—), 1594 (C═N), 1327, 1143 (SO_2CH_3) cm^1; ^{1}H NMR (DMSO-d_6, 400 MHz, δ, ppm): 3.28 (s, 3H, $SO_2\underline{CH_3}$), 7.47 (s, 1H, olefinic C—H), 7.62 (d, 2H, J = 8.4 Hz, methanesulfonylphenyl H-3, H-5), 7.66 (d, 2H, J = 8.4 Hz, 4-chlorophenyl H-2, H-6), 8.08 (d, 2H, J = 8.4 Hz, 4-chlorophenyl H-3, H-5), 8.28 (d, 2H, J = 8.4 Hz, methanesulfonylphenyl H-2, H-6), 8.81 (s, 1H, pyrazole H-5), 12.36 (s, 1H, NH, D_2O exchangeable); ^{13}C NMR (DMSO-d_6 100 MHz, δ, ppm): 44.76, 115.22, 117.46, 120.03, 129.00, 129.30, 129.56, 130.43, 130.83, 134.57, 139.34, 142.55, 144.22, 153.34, 167.22, 167.75; MS *m/z* (ES^+) 459 (M^+) (27.06%). Anal. Calcd. For $C_{20}H_{14}ClN_3O_4S_2$; C, 52.23; H, 3.07; N, 9.14; Found; C, 52.37; H, 3.16; N, 8.86.

*4.1.4.3. (E)-5-((3-(4-bromophenyl)-1-(4-(methylsulfonyl)phenyl)-1H-pyrazol-4-yl)methylene)-thiazolidine-2,4-dione (**12c**)*. Yield 46%; yellow solid; m.p. 205–207 °C; IR (KBr): 3244 (NH), 3057 (C—H aromatic), 2921 (C—H aliphatic), 1744, 1698 (C═O), 1615 (—CH═C—), 1593 (C═N), 1327, 1142 (SO_2CH_3) cm^1; ^{1}H NMR (DMSO-d_6, 400 MHz, δ, ppm): 3.26 (s, 3H, $SO_2\underline{CH_3}$), 7.44 (s, 1H, olefinic C—H), 7.56 (d, 2H, J = 8.4 Hz, methanesulfonylphenyl H-3, H-5), 7.73 (d, 2H, J = 8.4 Hz, 4-bromophenyl H-2, H-6), 8.05 (d, 2H, J = 8.4 Hz, 4-bromophenyl H-3, H-5), 8.23 (d, 2H, J = 8.4 Hz, methanesulfonylphenyl H-2, H-6), 8.75 (s, 1H, pyrazole H-5), 12.31 (s, 1H, NH, D_2O exchangeable); ^{13}C NMR (DMSO-d_6 100 MHz, δ, ppm): 44.23, 115.11, 117.22, 120.02, 123.21, 128.89, 129.32, 130.81, 131.07, 132.46, 139.22, 153.35, 155.22, 157.34, 167.00, 167.45; MS *m/z* (ES^+) 573.84 (M^+). MS *m/z* (ES^+) 502 (M^+) (100%). Anal. Calcd. For: $C_{20}H_{14}BrN_3O_4S_2$: C, 47.63; H, 2.80; N, 8.33; Found; C, 47.15; H, 2.83; N, 8.44.

*4.1.4.4. (E)-5-((1-(4-(methylsulfonyl)phenyl)-3-(4-nitrophenyl)-1H-pyrazol-4-yl)methylene)-thiazolidine-2,4-dione (**12d**)*. Yield 52%; yellow solid; m.p. 212–214 °C; IR (KBr): 3244 (NH), 3116 (C—H aromatic), 2928 (C—H aliphatic), 1745, 1704 (C═O), 1617 (—CH═C—), 1594 (C═N), 1348, 1143 (SO_2CH_3) cm^1; ^{1}H NMR (DMSO-d_6, 400 MHz, δ, ppm): 3.27 (s, 3H, $SO_2\underline{CH_3}$), 7.38 (s, 1H, olefinic C—H), 7.92 (d, 2H, J = 8.0 Hz, methanesulfonylphenyl H-3, H-5), 8.07 (d, 2H, J = 7.6 Hz, 4-nitrophenyl H-2, H-6), 8.25 (d, 2H, J = 8.0 Hz, methanesulfonylphenyl H-2, H-6), 8.37 (d, 2H, J = 7.6 Hz, 4-nitrophenyl H-3, H-5), 8.74 (s, 1H, pyrazole H-5), 12.39 (s, 1H, NH, D_2O exchangeable); ^{13}C NMR (DMSO-d_6 100 MHz, δ, ppm): 44.77, 118.27, 118.58, 119.60, 128.79, 128.93, 129.14, 129.35, 129.46, 129.91, 130.07, 138.36, 139.26, 151.80, 167.36, 167.88; MS *m/z* (ES^+) 470 (M^+) (44%). Anal. Calcd. For $C_{20}H_{14}N_4O_6S_2$: C, 51.06; H, 3.00; N, 11.91; Found; C, 51.28; H, 3.18; N, 11.58.

*4.1.4.5. (E)-N-(4-(4-((2,4-dioxothiazolidin-5-ylidene)methyl)-1-(4-(methylsulfonyl)phenyl)-1H-pyrazol-3-yl)phenyl)methanesulfonamide (**12e**)*. Yield 36%; yellow solid; m.p. 202–204 °C; IR (KBr): 3203 (NH), 3050 (C—H aromatic), 2926 (C—H aliphatic), 1746, 1697 (C═O), 1613 (—CH═C—), 1594 (C═N), 1372, 1145 (SO_2CH_3) cm^1; ^{1}H NMR (DMSO-d_6, 400 MHz, δ, ppm): 3.10 (s, 3H, $SO_2\underline{CH_3}$), 3.29 (s, 3H, $NHSO_2\underline{CH_3}$), 3.40 (s, 1H, $\underline{NH}SO_2CH_3$, D_2O exchangeable), 7.39 (d, 2H, J = 7.6 Hz methanesulfonylphenyl H-2, H-6), 7.53 (s, 1H, olefinic C—H), 7.62 (d, 2H, J = 7.6 Hz, *N*-phenylmethanesulfonamide H-3, H-5), 8.09 (d, 2H, J = 7.6 Hz methanesulfonylphenyl H-3, H-5), 8.15 (d, 2H, J = 7.6 Hz, *N*-phenylmethanesulfonamide H-2, H-6), 8.80 (s, 1H, pyrazole H-5), 12.31 (s, 1H, NH, D_2O exchangeable); ^{13}C NMR (DMSO-d_6 100 MHz, δ, ppm): 43.59, 44.77, 119.20, 119.82, 119.95, 121.32, 129.26, 129.44, 129.63, 129.90, 130.21, 131.93, 139.30, 139.92, 154.24 167.36, 168.39; MS *m/z* (ES^+) 518 (M^+) (100%). Anal. Calcd. For $C_{21}H_{18}N_4O_6S_3$: C, 48.64; H, 3.50; N, 10.80; Found; C, 48.65; H, 3.38; N, 10.66.

*4.1.4.6. (E)-5-((3-(4-methoxyphenyl)-1-(4-(methylsulfonyl)phenyl)-1H-pyrazol-4-yl)methylene-)thiazolidine-2,4-dione (**12f**)*. Yield 33%; yellow solid; m.p. 208–210 °C; IR (KBr): 3222 (NH), 3114 (C—H aromatic), 2925 (C—H aliphatic), 1744, 1705 (C═O), 1613 (—CH═C—), 1594 (C═N), 1368, 1143 (SO_2CH_3) cm^1; ^{1}H NMR (DMSO-d_6, 400 MHz, δ, ppm): 3.26 (s, 3H, $SO_2\underline{CH_3}$), 3.42 (s, 3H, $O\underline{CH_3}$), 7.11 (d, 2H, J = 8.0 Hz, 4-methoxyphenyl H-3, H-5), 7.48 (s, 1H, olefinic C—H), 7.56 (d, 2H, J = 8.0 Hz, methanesulfonylphenyl H-2, H-6), 8.04 (d, 2H, J = 8.0 Hz, 4-methoxyphenyl H-2, H-6), 8.26 (d, 2H, J = 8.0 Hz, methanesulfonylphenyl H-3, H-5), 8.74 (s, 1H, pyrazole H-5), 12.29 (s, 1H, NH, D_2O exchangeable); ^{13}C NMR (DMSO-d_6 100 MHz, δ, ppm): 39.23, 44.24, 114.86, 118.39, 118.62, 119.76, 123.93, 127.55, 128.39, 129.41, 130.20, 130.45, 130.62, 138.96, 142.71, 154.39, 160.43; MS *m/z* (ES^+) 455 (M^+). MS *m/z* (ES^+) 455 (M^+) (88%). Anal. Calcd. For $C_{21}H_{17}N_3O_5S_2$: C, 55.37; H, 3.76; N, 9.22; Found; C, 55.69; H, 3.47; N, 9.38.

*4.1.5. General procedure for synthesis of the thiazolidinone derivatives (**13a-f**)*

To a hot solution of the appropriate pyrazole (**10a-f**) (2 mmol) in glacial acetic acid (20 mL) (2.0 mmol) chloroacetic acid was added with (2.0 mmol) of anhydrous sodium acetate. The reaction mixture was heated under reflux for 24 h, the formed precipitate was filtered and recrystallized from ethanol to give the final derivatives (**13a-f**). Physical and spectral data are listed below:

*4.1.5.1. (E)-2-((E)-((1-(4-(methylsulfonyl)phenyl)-3-phenyl-1H-pyrazol-4-yl)methylene)hydrazono-)thiazolidin-4-one (**13a**)*. Yield 39%; white solid; m.p. 256–258 °C; IR (KBr): 3225 (NH), 3017 (C—H aromatic), 2926 (C—H aliphatic), 1717 (C═O), 1643 (—CH═C—), 1593 (C═N), 1317, 1142 (SO_2CH_3) cm^1; ^1H NMR (DMSO-d_6, 400 MHz, δ, ppm): 3.29 (s, 3H, $SO_2\underline{CH_3}$), 3.92 (s, 2H, CH_2 of thiazolidinone ring), 7.51 (m, 3H, phenyl H-3, H-4, H-5), 7.86 (d, 2H, J = 7.6 Hz, phenyl H-2, H-6), 8.09 (d, 2H, J = 8.0 Hz, methanesulfonylphenyl H-3, H-5), 8.27 (d, 2H, J = 8.0 Hz, methanesulfonylphenyl H-2, H-6), 8.43 (s, 1H, olefinic C—H), 9.14 (s, 1H, pyrazole H-5), 12.23 (s, 1H, NH, D_2O exchangeable); ^{13}C NMR (DMSO- d_6 100 MHz, δ, ppm): 39.76, 44.06, 118.12, 119.54, 129.02, 129.18, 129.34, 129.42, 129.54, 130.96, 132.11, 139.08, 142.73, 149.30, 153.01, 167.85; MS m/z (ES^+) 439 (M+) (88%). Anal. Calcd. For $C_{20}H_{17}N_5O_3S_2$: C, 54.56; H, 3.90; N, 15.93; Found; C, 54.76; H, 3.99; N, 15.79.

*4.1.5.2. (E)-2-((E)-((3-(4-chlorophenyl)-1-(4-(methylsulfonyl)phenyl)-1H-pyrazol-4-yl)methylene)-hydrazono)thiazolidin-4-one (**13b**)*. Yield 42%; white solid; m.p. 180–182 °C; IR (KBr): 3421 (NH), 3017 (C—H aromatic), 2931 (C—H aliphatic), 1711 (C═O), 1644 (—CH═C—), 1593 (C═N), 1318, 1143 (SO_2CH_3) cm^1; ^1H NMR (DMSO-d_6, 400 MHz, δ, ppm): 3.26 (s, 3H, $SO_2\underline{CH_3}$), 3.94 (s, 2H, CH_2 of thiazolidinone ring), 7.53 (d, 2H, J = 8.4 Hz, methanesulfonylphenyl H-3, H-5), 7.93 (d, 2H, J = 8.0 Hz, 4-chlorophenyl H-2, H-6), 8.06 (d, 2H, J = 8. Hz, 4-chlorophenyl H-3, H-5), 8.20 (d, 2H, J = 8.4 Hz, methanesulfonylphenyl H-2, H-6), 8.42 (s, 1H, olefinic C—H), 9.10 (s, 1H, pyrazole H-5), 12.26 (s, 1H, NH, D_2O exchangeable); ^{13}C NMR (DMSO-d_6 100 MHz, δ, ppm): 33.76, 49.05, 118.15, 129.35, 129.41, 130.60, 131.05, 132.11, 134.04, 134.35, 138.99, 142.56, 142.66, 153.26, 165.45, 174.27; MS m/z (ES^+) 473 (M^+) (100%). Anal. Calcd. For $C_{20}H_{16}ClN_3O_3S_2$; C, 50.68; H, 3.40; N, 14.78; Found; C, 50.37; H, 3.16; N, 14.86.

*4.1.5.3. (E)-2-((E)-((3-(4-bromophenyl)-1-(4-(methylsulfonyl)phenyl)-1H-pyrazol-4-yl)methylene)-hydrazono)thiazolidin-4-one (**13c**)*. Yield 36%; white solid; m.p. 183–185 °C; IR (KBr): 3431 (NH), 3057 (C—H aromatic), 2925 (C—H aliphatic), 1722 (C═O), 1637 (—CH═C—), 1594 (C═N), 1320, 1144 (SO_2CH_3) cm^1; ^1H NMR (DMSO-d_6, 400 MHz, δ, ppm): 3.28 (s, 3H, $SO_2\underline{CH_3}$), 3.91 (s, 2H, CH_2 of thiazolidinone ring), 7.46 (d, 2H, J = 8.4 Hz, methanesulfonylphenyl H-3, H-5), 7.74 (d, 2H, J = 8.4 Hz, 4-bromophenyl H-2, H-6), 7.88 (d, 2H, J = 8.4 Hz, 4-bromophenyl H-3, H-5), 8.21 (d, 2H, J = 8.4 Hz, methanesulfonylphenyl H-2, H-6), 8.42 (s, 1H, olefinic C—H), 9.10 (s, 1H, pyrazole H-5), 11.95 (s, 1H, NH, D_2O exchangeable); ^{13}C NMR (DMSO-d_6 100 MHz, δ, ppm): 33.75, 44.04, 115.01, 118.15, 122.75, 123.04, 129.34, 130.93, 131.36, 132.33, 139.04, 142.56, 149.23, 153.27, 165.36, 174.28; MS m/z (ES^+) 573.84 (M^+). MS m/z (ES^+) 516 (M^+) (100%). Anal. Calcd. For: $C_{20}H_{16}BrN_5O_3S_2$: C, 46.34; H, 3.11; N, 13.51; Found; C, 46.15; H, 3.44; N, 13.24.

*4.1.5.4. (E)-2-((E)-((1-(4-(methylsulfonyl)phenyl)-3-(4-nitrophenyl)-1H-pyrazol-4-yl)methylene-)hydrazono)thiazolidin-4-one (**13d**)*. Yield 42%; white solid; m.p. 212–214 °C; IR (KBr): 3261 (NH), 3116 (C—H aromatic), 2921 (C—H aliphatic), 1713 (C═O), 1596 (—CH═C—), 1534 (C═N), 1344, 1154 (SO_2CH_3) cm^1; ^1H NMR (DMSO-d_6, 400 MHz, δ, ppm): 3.30 (s, 3H, $SO_2\underline{CH_3}$), 3.62 (s, 2H, CH_2 of thiazolidinone ring), 7.99 (d, 2H, J = 8.4 Hz, methanesulfonylphenyl H-3, H-5), 8.12 (d, 2H, J = 8.4 Hz, 4-nitrophenyl H-2, H-6), 8.17 (d, 2H, J = 8.4 Hz, methanesulfonylphenyl H-2, H-6), 8.28 (s, 1H, olefinic C—H), 8.35 (d, 2H, J = 8.4 Hz, 4-nitrophenyl H-3, H-5), 9.38 (s, 1H, pyrazole H-5), 11.42 (s, 1H, NH, D_2O exchangeable); ^{13}C NMR (DMSO-d_6 100 MHz, δ, ppm):35.14, 44.05, 119.46, 119.59, 123.92, 124.20, 124.41, 129.37, 129.70, 130.30, 132.48, 139.16, 142.47, 147.60, 149.92, 167.13; MS m/z (ES^+) 470 (M^+) (44%). Anal. Calcd. For $C_{20}H_{16}N_6O_5S_2$: C, 49.58; H, 3.33; N, 17.35; Found; C, 49.28; H, 3.18; N, 17.58.

*4.1.5.5. N-(4-(1-(4-(methylsulfonyl)phenyl)-4-((E)-((E)-(4-oxothiazolidin-2-ylidene)hydrazono)methyl)-1H-pyrazol-3-yl)phenyl) methanesulfonamide (**13e**)*. Yield 32%; white solid; m.p. 176–178 °C; IR (KBr): 3203 (NH), 3016 (C—H aromatic), 2931 (C—H aliphatic), 1731 (C═O), 1639 (—CH═C—), 1594 (C═N), 1344, 1151 (SO_2CH_3) cm^1; ^1H NMR (DMSO-d_6, 400 MHz, δ, ppm): 3.35 (s, 3H, $SO_2\underline{CH_3}$), 3.59 (s, 3H, $NHSO_2\underline{CH_3}$), 3.88 (s, 1H, $\underline{NH}SO_2CH_3$, D_2O exchangeable), 3.90 (s, 2H, CH_2 of thiazolidinone ring), 7.65 (d, 2H, J = 8.0 Hz methanesulfonylphenyl H-2, H-6), 8.02 (d, 2H, J = 8.0 Hz, *N*-phenylmethanesulfonamide H-3, H-5), 8.21 (d, 2H, J = 8.0 Hz methanesulfonylphenyl H-3, H-5), 8.46 (d, 2H, J = 8.0 Hz, *N*-phenylmethanesulfonamide H-2, H-6), 8.49 (s, 1H, olefinic C—H), 9.19 (s, 1H, pyrazole H-5), 11.88 (s, 1H, NH, D_2O exchangeable); ^{13}C NMR (DMSO-d_6 100 MHz, δ, ppm): 33.70, 44.03, 118.39,119.33, 119.60, 129.37, 130.27, 131.59, 131.77, 132.03, 134.03, 134.56, 139.24, 142.64, 149.02, 151.64, 167.36; MS m/z (ES^+) 518 (M^+) (100%). Anal. Calcd. For $C_{21}H_{20}N_6O_5S_3$: C, 47.36; H, 3.78; N, 15.78; Found; C, 47.65; H, 3.38; N, 15.66.

*4.1.5.6. (E)-2-((E)-((3-(4-methoxyphenyl)-1-(4-(methylsulfonyl)phenyl)-1H-pyrazol-4-yl)methylene)-hydrazono)thiazolidin-4-one (**13f**)*. Yield 41%; white solid; m.p. 236–238 °C; IR (KBr): 3225 (NH), 3116 (C—H aromatic), 2931 (C—H aliphatic), 1723 (C═O), 1644 (—CH═C—), 1594 (C═N), 1326, 1141 (SO_2CH_3) cm^1; ^1H NMR (DMSO-d_6, 400 MHz, δ, ppm): 3.28 (s, 3H, $SO_2\underline{CH_3}$), 3.82 (s, 3H, $O\underline{CH_3}$), 3.88 (s, 2H, CH_2 of thiazolidinone ring), 7.06 (d, 2H, J = 8.0 Hz, 4-methoxyphenyl H-3, H-5), 7.82 (d, 2H, J = 8.0 Hz, methanesulfonylphenyl H-2, H-6), 8.08 (d, 2H, J = 8.0 Hz, 4-methoxyphenyl H-2, H-6), 8.24 (d, 2H, J = 8.0 Hz, methanesulfonylphenyl H-3, H-5), 8.40 (s, 1H, olefinic C—H), 9.07 (s, 1H, pyrazole H-5), 12.29 (s, 1H, NH, D_2O exchangeable); ^{13}C NMR (DMSO-d_6 100 MHz, δ, ppm): 39.79, 44.50, 55.70, 114.41, 114.95, 117.88, 119.79, 124.13, 124.45, 130.68, 130.88, 138.82, 142.73, 142.82, 144.67, 164.78, 174.91; MS m/z (ES^+) 469 (M^+) (81%). Anal. Calcd. For $C_{21}H_{19}N_5O_4S_2$: C, 53.72; H, 4.08; N, 14.92; Found; C, 53.69; H, 4.47; N, 15.30.

4.2. Biological evaluation

4.2.1. Ant-inflammatory

4.2.1.1. In vitro cyclooxygenase inhibition assay. The ability of the target compounds **12a-f** and **13a-f** to inhibit ovine COX-1 and human recombinant COX-2 (IC_{50} value, μM) was determined using an enzyme immuno assay (EIA) kit (catalog no. 560131, Cayman Chemical, Ann Arbor, MI, USA) according to the previously reported procedure [40].

4.2.1.2. In vivo anti-inflammatory assay. The target thiazolidindione s **12a-f**, thiazolidinones **13a-f** and the reference drug celecoxib were evaluated for their anti-inflammatory activities using the *in vivo* carrageenan-induced rat foot paw edema model (50 mg/kg) and the measurement of paw thickness was done after 1, 3 and 5 h of carageenan injection as reported before [41]. Additionally, the dose causing 50% edema inhibition (ED_{50}) was determined for the most potent AI derivatives **12b**, **12bc**, **12f**, **13b**, **13c**, **13e** and **13f** in comparison to celecoxib [41].

4.2.1.3. Ulcerogenic liability. Ulcerogenic liability of the most potent AI derivatives **12b**, **12bc**, **12f**, **13b**, **13c**, **13e** and **13f** in comparison to low ulcerogenic drug (celecoxib) and high ulcerogenic drug (ibuprofen) was evaluated using 50 mg/kg dose according to the reported procedure [42].

4.2.2. Ant-diabetic activity

4.2.2.1. In vitro α-glucosidase/β-glucosidase inhibitory activity. The assay of α-glucosidase inhibitory activity was performed as previously described [43] with some modifications. A volume of 25 µL of varying concentrations of the synthetic compounds (0.1, 0.2, 0.3, 0.4, and 0.5 mg/ml) was added to 96 well plate containing a mixture of 50 µL phosphate buffer (100 mM, pH = 6. 8) and 10 µL alpha-glucosidase (1 U/ml) and the mixture was first incubated at 37 °C for 20 min followed by another 20 min incubation after addition of 25 µL of 5 mM P-NPG (substrate). The reaction was stopped by adding 50 µL Na CO (0.1 M). The absorbance of the released p-nitrophenol was measured at 405 nm using Microplate Reader. Acarbose at various concentrations (0.1–0.5 mg/ml) was included as a standard. Without test substance was set up in parallel as a control and each experiment was performed in triplicates. The results were expressed as percentage inhibition, which was calculated using the formula, Inhibitory activity (%) = (1 − At/Ac) × 100, where, "At" is the absorbance in the presence of test substance and "Ac" is the absorbance of control.

Moreover, B-glucosidase inhibitory activity was assayed using p-nitrophenyl-β-D-glucopyranoside (pNPG) by micro titer plate method as described [44]. A reaction mixture (100 µL) containing 25 µL of enzyme, 25 µL of pNPG (10 mM) as substrate and sodium acetate buffer (50 mM, pH 5.0) was incubated at 50 °C for 30 min, the reaction was terminated by addition of 100 µL of NaOH-glycine buffer (0.4 M, pH 10.8). The developed yellow color was read at 405 nm using ELISA Reader. The amount of *p*-nitrophenol released was quantified using the pNP standard. One unit of β-glucosidase activity was expressed as the amount of enzyme required to release 1 µmole of pNP per minute under the assay conditions. Without test substance was set up in parallel as a control and each experiment was performed in triplicates. The results were expressed as percentage inhibition, which was calculated using the formula, Inhibitory activity (%) = (1 − At/Ac) ×100, where, At is the absorbance in the presence of test substance and Ac is the absorbance of control.

4.2.2.2. In vitro PPAR-γ activation. Normal kidney cell line, Vero, was cultured in 96-wells plate (60000 cells/well) containing Dulbecco's Modified Eagle Medium (DMEM) supplemented with 10% fetal bovine serum. The cells were incubated in 5% CO2 incubator at 37 °C till reaching 70–80% confluence and then they were transfected with 2.5 µL of PPRE-Luciferase, 6.67 µL of PPARγ. Five hours after transfection, the cells were treated with synthesized compounds (10 µM) for 24 h and then collected with cell culture lysis buffer. Pioglitazone and Rosiglitazone were used as reference drugs and Luciferase activity was monitored using the luciferase assay kit according to manufacturer's instructions (Promega).

4.2.2.3. In vivo hypoglycemic study

4.2.2.3.1. Animals and treatment. Wistar Albino rats of either sex weighing between 150 and 200 gm were kept on overnight fasting and had free access to water. Blood samples were collected by tail tapping method and the initial fasting blood glucose was estimated by digital glucometer. Animals were made diabetic by single tail vein injection of alloxan (60 mg/kg). Dextrose 5% solution was administered via feeding bottle, to recover from early hypoglycemic phases. After 48 hrs, the blood was withdrawn by tail tapping method and blood glucose level was estimated. The animals showing blood glucose levels above 250 mg/dL were selected for study and divided into experimental groups of 4 animals each. Thus, it was concluded that hyperglycemia was induced within 48 hrs and stabilized within 5 days [45].

4.2.2.3.2. One day study. Diabetic control Group (Group 1) received distilled water only. (Group 2) animals were orally fed with rosiglitazone 30 mg/kg. (Group 3–Group 14) animals were given the synthesized compounds orally (homogenized suspension in 0.25% carboxymethyl cellulose (CMC)) and screened for hypoglycemic activity at a fixed dose of 50 mg/kg body weight, *in vivo* alloxan induced diabetic rat model for one day study animals were fasted overnight and the fasting blood glucose, 0 hr, levels were observed. Blood samples were removed from all animals at 0, 2, 4, 6 and 12 hrs. The data obtained was analyzed by one-way ANOVA followed by Dunnett test. The results were expressed as mean ± standard error of mean (SEM) for each group, $p < 0.0001$ was considered as statistically significant and the results are explained in Table 7.

4.2.2.3.3. Fifteen days study. Study animals were fasted overnight and the fasting blood glucose, levels were calculated. Now the tested compounds were administered at a fixed dose of 50 mg/kg orally (homogenized suspension in 0.25% CMC) for 15 days daily at a fixed time. After 15 days treatment was stopped and blood glucose level was measured, after 30 min of the administration of the last dose. During study, blood samples were removed from all animals at 7, 15 days and change in blood glucose was calculated. The data obtained was analyzed by one-way ANOVA followed by Dunnett test. The results were expressed as mean ± standard error of mean (SEM) for each group, $p < 0.0001$ was considered as statistically significant.

4.3. Molecular modeling

4.3.1. Shape alignment and scoring using ROCS

Basic method to represent shape and color features in ROCS is using ROCs application Open Eye scientific software. Celecoxib and rosiglitazone were selected as query molecules. Compounds library was adopted as the database file. Both query and database files were energy minimized by Omega applications Open Eye scientific software. ROCS runs were employed by personal PC in very fast using vROCS interface. vROCS was employed to run and analyze/visualize the results. ROCS application searched the database with the query to find molecules with similar shape and colors. Compounds conformers were scored based upon the Gaussian overlap to the query and the best scoring parameters is Tanimoto Combo scores (shape + color), the highest score is the best matched with query compound 46–48].

4.3.2. Molecular docking study

The docking studies were performed using the OpenEye Modeling software [50–52]. A virtual library of target compounds was used and their energies were minimized using the MMFF94 force field, followed by the generation of multi-conformers using the OMEGA application. The whole library of minimized energy values was docked appropriate target with reported cocrystalized standard. The receptor PDB files were downloaded from the Protein Data Bank (PDB). For anti-inflammatory action, docking was employed with COX-2 (PDB ID: 3LN1) [49] while for anti-diabetic activity, compounds docked with PPARγ (PDB ID: 4O8F) [53]. Both the ligand input file and the receptor input file were passed into FRED to perform the molecular docking simulations. Multiple scoring functions were employed to predict energy profile of the ligand-receptor complex. The vida application was employed as a visualization tool to show the ligands pose and the potential binding interactions of the ligands to the receptor of interest.

Acknowledgments

The authors acknowledge OpenEye Scientific Software Inc. (Santa Fe, NM, USA) for providing the academic license.

Conflict of interest

The authors have declared no conflict of interest

Appendix A. Supplementary material

Supplementary data to this article can be found online at https://doi.org/10.1016/j.bioorg.2018.09.034.

References

[1] World Health Organization, Global Report on Diabetes. Geneva, 2016. <http://www.who.int/diabetes/global-report/en/> (accessed 30 August, 2016).
[2] A.A.O. Abeed, M.S.K. Youssef, R. Hegazy, J. Braz. Chem. Soc. 28 (11) (2017) 2054–2063.
[3] S. Sen, B. De, T.S. Easwar, Trop. J. Pharm. Res. 13 (2014) 1445–1454.
[4] S.A. Kliewer, H.E. Xu, M.H. Lambert, T.M. Willson, Recent Prog. Horm. Res. 56 (2000) 239–263.
[5] G.Q. Shi, J.F. Dropinski, B.M. McKeever, S. Xu, J.W. Becker, J.P. Berger, K.L. MacNaul, A. Elbrecht, G. Zhou, T.W. Doebber, P. Wang, J. Med. Chem. 48 (2005) 4457–4468.
[6] M.J. Naim, M.J. Alam, S. Ahmad, F. Nawaz, N. Shrivastava, M. Sahu, O. Alam, Eur. J. Med. Chem. 129 (2017) 218–250.
[7] M.J. Naim, M.J. Alam, F. Nawaz, V.G.M. Naidu, S. Aaghaz, M. Sahu, N. Siddiqui, O. Alam, Bioorg. Chem. 73 (2017) 24–36.
[8] M.J. Naim, O. Alam, M.J. Alam, M. Shaquiquzzaman, M.M. Alam, V.G.M. Naidu, Arch. Pharm. (Weinheim) 351 (2018) 3–4.
[9] M.C. Unlusoy, C. Kazak, O. Bayro, E.J. Verspohl, R. Ertan, O.B. Dundar, J. Enzyme Inhib. Med. Chem. 28 (2013) 1205–1210.
[10] P. Neogi, J. Cheng, F.J. Lakner, D. Dey, S. Medicherla, M. Gowri, B. Nag, S.D. Sharma, L.B. Pickford, C. Gross, Bioorg. Med. Chem. 11 (2003) 4059–4067.
[11] A.P.G. Nikalje, S. Choudhari, H. Une, Eur. J. Exp. Biol. 2 (2012) 1302–1314.
[12] P.A. Datar, S.B. Aher, J. Saudi Chem. Soc. 20 (2016) S196–S201.
[13] S. Nazreen, M.S. Alam, H. Hamid, M.S. Yar, S. Shafi, A. Dhulap, P. Alam, M.A.Q. Pasha, S. Bano, M.M. Alam, S. Haider, Y. Ali, C. Kharbanda, Eur. J. Med. Chem. 87 (2014) 175–185.
[14] H. Yki-Jarvinen, Thiazolidindione s, N. Engl. J. Med. 351 (2004) 1106–1118.
[15] G.J. Murphy, J.C. Holder, Trends Pharmacol. Sci. 21 (2000) 469–474.
[16] A. Consoli, E. Devangelio, Lupus 14 (2005) 794–797.
[17] J.F. Navarro, C. Mora, Sci. World J. 6 (2006) 908–917.
[18] S. arcia-Vallv, L. Guasch, S. Tomas-Hern Ndez, J.M. del Bas, V. Ollendorff, L. Arola, G. Pujadas, M. Mulero, J. Med. Chem. 58 (2015) 5381–5394.
[19] J.M. Olefsky, A.R. Saltiel, Diabetes 45 (1996) 1661–1669.
[20] J. Benardeau, A. Benz, D. Binggeli, M. Blum, U. Boehringer, H. Grether, B. ilpert, H.P. Kuhn, M. Marki, K. Meyer, S. Puntener, A. Raab, D. Ruf, P Mohr Schlatter, Aleglitazar, Bioorg. Med. Chem. Lett. 19 (2009) 2468–2473.
[21] S. Seto, K. Okada, K. Kiyota, S. Isogai, M. Iwago, T. Shinozaki, Y. Kitamura, Y. Kohno, K. Murakami, J. Med. Chem. 53 (2010) 5012–5024.
[22] B. Spiegelman, Diabetes 47 (1998) 507–514.
[23] M. Ahmadian, J.M. Suh, N. Hah, C. Liddle, A.R. Atkins, M. Downes, R.M. Evans, Nat. Med. 99 (2013) 557–566.
[24] L. Fuentes, T. Roszer, M. Ricote, Mediat. Inflamm. 219583 (2010), https://doi.org/10.1155/2010/219583.
[25] C. Blanquart, O. Barbier, J.C. Fruchart, B. Staels, C. Glineur, J. Steroid Biochem. 85 (2003) 267–273.
[26] C. Jiang, A.T. Ting, B. Seed, Nature 391 (1998) 82–86.
[27] M. Ricote, A.C. Li, T.M. Willson, C.J. Kelly, C.K. Glass, Nature 391 (1998) 79–82.
[28] Q.-L. Bo, Y.-H. Chen, Z. Yu, L. Fu, Y. Zhou, G.-B. Zhang, H. Wang, Z.-H. Zhang, D. Xu, Mol. Cell. Endocrinol. 423 (2016) 51–59.
[29] S. Fiorucci, R. Meli, M. Bucci, G. Cirino, Biochem. Pharmacol. 62 (2013) 1433–1438.
[30] K.R.A. Abdellatif, M.A. Chowdhury, Y. Dong, C. Velázquez, D. Das, M.R. Suresh, E.E. Knaus, Bioorg. Med. Chem. 16 (2008) 9694–9698.
[31] T.D. Penning, J.J. Tally, S.R. Bertenshaw, J.S. Carter, P.W. Collins, S. Doctor, M.J. Graneto, L.F. Lee, J.W. Malecha, J.M. Miyashiro, R.S. Rogers, D.J. Rogier, S.S. Yu, G.D. AndersonBurton, E.G. Cogburn, J.N. Gregory, C.M. Koboldt, W.E. Perkins, K. Seibert, A.W. Veenhuizen, Y.Y. Zhang, P.C. Isakson, J. Med. Chem. 40 (1997) 1347–1365.
[32] P. Prasit, Z. Wang, C. Brideau, C.C. Chan, S. Charleson, W. CromLish, D. Ethier, J.F. Evans, A.W. Ford-Hutchinson, J.Y. Gauthier, R. Gordon, J. Guay, M. Gresser, S. Kargman, B. Kennedy, Y. Leblanc, S. Leger, J. Mancini, G.P. O'Neill, M. Quellet, M.D. Percival, H. Perrier, D. Riendeau, I. Rodger, P. Tagari, M. Therien, P. Vickers, E. Wong, L.J. Xu, R.N. Young, R. Zamboni, S. Boyce, N. Rupniak, M. Forrest, D. Visco, D. Patrick, Bioorg. Med. Chem. Lett. 9 (1999) 1773–1778.
[33] C.V. Junior, A. Danuello, V.D.S. Bolzani, E.J. Barreiro, C.A.M. Fraga, Curr. Med. Chem. 14 (2007) 1829–1852.
[34] L.K. Gediya, V.C. Njar, Expert Opin. Drug, Discovery 4 (2009) 1099–1111.
[35] K.R.A. Abdellatif, W.A.A. Fadaly, G.M. Kamel, J. Enz. Inhib. Med. Chem. 31 (3) (2016) 54–60.
[36] K.R.A. Abdellatif, M.A. Abdelgawad, H.A.H. Elshemy, S.S.R. Alsayed, Bioorg. Chem. 64 (2016) 1–12.
[37] K.R.A. Abdellatif, W.A.A. Fadaly, Bioorg. Chem. 70 (2017) 57–66.
[38] K.R.A. Abdellatif, W.A.A. Fadaly, Bioorg. Chem. 72 (2017) 123–129.
[39] K.R.A. Abdellatif, W.A.A. Fadaly, Y.A.M.M. Elshaier, W.A.M. Ali, G.M. Kamel, Bioorg. Chem. 77 (2018) 568–578.
[40] B. Roschek, R.C. Fink, D. Li, M. McMichael, C.M. Tower, R.D. Smith, R.S. Alberte, J. Med. Food 12 (2009) 615–625.
[41] C.A. Winter, E.A. Risley, G.W. Nuss, Exp. Biol. Medi. 111 (3) (1962) 544–547.
[42] G.S. Hassan, S.M. Abou-Seri, G. Kamel, M.M. AliEur, J. Med. Chem. 76 (2014) 482–493.
[43] L.J. Shai, S.R. Magano, S.L. Lebelo, A.M. Mogale, J. Med. Plant Res. 5 (2011) 2863–2867.
[44] N.J. Parry, D.E. Beever, E. Owen, I. Vandenberghe, J.V. Beeumen, M.K. Bhat, Biochem. J. 353 (2001) 117–127.
[45] R. Murugan, S. Anbazhagan, S. Narayanan, Eur. J. Med. Chem. 44 (2009) 3272–3279.
[46] ROCS, Shape Similarity for Virtual Screening & Lead Hopping; <https://www.eyesopen.com/rocs>.
[47] P.C.D. Hawkins, A.G. Skillman, A. Nicholls, J. Med. Chem. 50 (2007) 74–82.
[48] J.J. Sutherland, R.K. Nandigam, J.A. Erickson, M. Vieth, J. Chem. Inf. Model 49 (2007) 2293–2302.
[49] J.L. Wang, D. Limburg, M.J. Graneto, J. Springer, J.R.B. Hamper, S. Liao, J.L. Pawlitz, R.G. Kurumbail, T. Maziasz, J.J. Talley, Bioorg. Med. Chem. lett. 20 (23) (2010) 7159–7163.
[50] Fast Rigid Exhaustive Docking (FRED) Receptor, version 2.2.5, OpenEye Scientific Software, Santa Fe, NM (USA). <http://www.eyesopen.com>.
[51] OMEGA, version 2.5.1.4; OpenEye Scientific Software, Santa Fe, NM (USA), <http://www.eyesopen.com>.
[52] VIDA, version 4.1.2; OpenEye Scientific Software, Santa Fe, NM (USA), <http://www.eyesopen.com>.
[53] C. Lori, A. Pasquo, R. Montanari, D. Capelli, V. Consalvi, R. Chiaraluce, L. Cervoni, F. Loiodice, A. Laghezza, M. Aschi, A. Giorgi, G. Pochetti, Acta Crystallogr. Sect.D 70 (2014) 1965–1976.
[54] A. Lee, L. Tan, H. Yang, G. Im, J. Im, Sci. Rep. 7 (2017) 16837 16837.